



Report on solutions to provide virtual inertia to islands' grids

Deliverable D5.2



This project has received funding from the European Union's Horizon 2020 research and innovation programme under grant agreement No. 957843 (MAESHA). This output reflects only the author's view, and the European Union cannot be held responsible for any use that may be made of the information contained therein

Deliverable **D5.2**

**REPORT ON SOLUTIONS TO PROVIDE VIRTUAL INERTIA TO
ISLANDS' GRIDS**



Organisation: **COBRA**

Main authors: **Daniel Rayo (COBRA), Evelyn Heylen (CENTRICA)**

Date (31/10/2022)

DELIVERABLE 5.2 – VERSION 1

WORK PACKAGE N° 5

Nature of the deliverable		
R	Document, report (excluding the periodic and final reports)	x
DEC	Demonstrator, pilot, prototype, plan designs	
DEM	Websites, patents filing, press & media actions, videos, etc.	
O	Software, technical diagram, etc.	

Dissemination level		
PU	Public	x
CO	Confidential, restricted under conditions set out in Model Grant Agreement	
CI	Classified, information as referred to in Commission Decision 2001/844/EC	

Quality procedure

Revision	Date	Created by	Short Description of Changes
1	30/09/2022	COBRA	Initial version of the document
2	01/10/2022	COBRA	Integration of contributions from T5.2 partners.
3	31/10/2022	COBRA	Preliminary version
4	30/11/2022	CENTRICA/COBRA	First review based on reviews comments
5	13/12/2022	COBRA	Final version

Document Approver(s) and Reviewer(s):

NOTE: All Approvers are required. Records of each approver must be maintained. All Reviewers in the list are considered required unless explicitly listed as Optional.

Name	Role	Action	Date
Vladimir Vrabel	WP5 leader	Review	14/10/2022
Christoph Gutschi	Reviewer	Review	21/10/2022
Tim Ronan Britton	Reviewer	Review	04/11/2022

ACKNOWLEDGEMENT

This project has received funding from the European Union's Horizon 2020 research and innovation programme under grant agreement No. 957843 (MAESHA). This output reflects only the author's view and the European Union cannot be held responsible for any use that may be made of the information contained therein.

More information on the project can be found at <https://www.maesha.eu>

EXECUTIVE SUMMARY

This report is oriented to evaluate current solutions to provide virtual inertia on islands' power systems. Besides conventional synchronous generators for grid stabilization, new solutions are available on the market. Some of them are explored in this document, differentiating among those based on rotating masses – flywheels and kinetic inertia from wind turbines – and those based on virtual inertia generators – grid-forming inverters –. The following table summarizes the main characteristics of each technology.

Technology	Price	Main-tain	Performance	Constrains	State of development
Flywheels	High (~80 k€/MW)	Low	90-95%	High power but limited energy	Commercially available
Kinetic inertia from wind turbines	Low (additional hardware is not required)	Low	Very high (only mechanical losses)	Provision of inertia implies angular velocity reduction, and output power drop	Test under real environment
Grid forming inverters	Low-Medium (higher than grid following inverters)	Low	Very high (~98%)	Limited deployment and untested performance in large power system	Advanced test on microgrids

Based on this table, grid-forming inverters, connected to variable renewable sources or storage technologies (batteries), constitutes one of the most promising solutions for guaranteeing renewable penetration in the power system with a stable and secure grid. Its limited cost, high efficiency, low maintenance costs, and promising results position this technology as a very good alternative for complementing against the current function of synchronous generators.

These solutions will be very valuable for the island of Mayotte, where a quick change in renewable penetration could cause some grid instabilities. If properly analysed, this could be avoided, or minimized through different strategies like virtual inertia implementation. In detail, one of the most promising solutions, battery storage system, has an average cost of 5,1 €/kW/a for a total useful life of 20 years, with a CAPEX of 101 €/kW. This cost represents around the 10% of the CAPEX associated of a new PW or Wind farm power plant, in terms of €/kW installed.

Moreover, this document reinforces the need of incorporating new solutions of inertia due to, according to the estimations carried out on it, the underfrequency load-shedding limit which would be reached in a range of 0,255 s to 0,72 s, if the power system was to lose the largest power plant

(11MW). In addition, this scenario would get worst progressively if the new renewable sources introduced in the island are not adapted to the inertia and grid stability requirements.

Furthermore, this document includes some examples of research and pilot projects for demonstrating the positive impact of different inertia systems in their respective power systems. In addition, a use case focused on evaluating the hypothetical use of a BESS for virtual inertia and energy arbitrage has been analysed from an economic point of view. This concludes that if the virtual inertia price rises beyond €15/MW/h, the BESS owner should reserve at least 98% of the total BESS power capacity for virtual inertia.

TABLE OF CONTENTS

ACKNOWLEDGEMENT	4
TABLE OF CONTENTS	7
LIST OF FIGURES	8
LIST OF TABLES	9
LIST OF ACRONYMS	10
1. INTRODUCTION	11
2. INERTIA IN GRID SYSTEMS AND POWER QUALITY	12
2.1. REGULATION IN THE EU	13
3. CASE STUDY – SPECIFIC TO MAYOTTE’S POWER GRID	16
3.1. CHARACTERISTICS OF MAYOTTE’S POWER GRID	16
3.2. FINDINGS OF PRECEDING TASKS IN MAESHA	17
4. TECHNOLOGIES AND SOLUTIONS TO INCREASE INERTIA IN GRIDS. MARKET REVIEW.	19
4.1. TECHNOLOGIES BASED ON ROTATIONAL INERTIA	19
4.2. TECHNOLOGIES ANALYSIS BASED ON POWER ELECTRONICS (GRID-FORMING AND GRID-FOLLOWING INVERTERS)	21
4.3. VIRTUAL INERTIAL TOPOLOGIES	23
4.4. DEVELOPED PROJECTS AND EXAMPLES OF APPLICATION	26
4.5. COST COMPETITIVENESS ANALYSIS AND MARKET VALUE OF GRID STABILIZATION	28
5. THE ROLE OF VIRTUAL INERTIA IN SYSTEM STABILITY	32
5.1. MANAGING FREQUENCY STABILITY AROUND THE WORLD	32
5.2. ADDED VALUE OF VIRTUAL INERTIA FOR FREQUENCY STABILITY	33
6. ECONOMIC ASSESSMENT OF DELIVERY OF A VIRTUAL INERTIA PRODUCT WITH A BATTERY ENERGY STORAGE SYSTEM	36
6.1. METHODOLOGY	36
6.2. RESULTS	40
7. CONCLUSIONS	44
8. REFERENCES	46

LIST OF FIGURES

Figure 1. Future direction in the power systems distributions (NREL, Research Roadmap on Grid-Forming Inverters, 2020)	12
Figure 2. Concept of virtual or synthetic inertia (internal).....	13
Figure 3. Frequency control mechanisms (Fei Teng, 2016).....	15
Figure 4. Flywheel scheme (Pullen, 2020).....	19
Figure 5. Schematic for frequency droop control (Ujjwol Tamrakar, 2017).	24
Figure 6. Synchronverter topology: (a) overall schematic showing operating principle; (b) detailed control diagram showing the modelling equations (Ujjwol Tamrakar, 2017).	24
Figure 7. Implementation of VOC on a single-phase H-bridge inverter with an LCL filter (CALIFORNIA, 2018).	25
Figure 8. Specific annual cost of inertia for wind, battery, and synchronous flywheel configurations [17].	30
Figure 9. Capital cost comparison for renewable and conventional energy sources (LAZARD, 2021).	31
Figure 10. Costs spent on ROCOF management by National Grid between April 1 and September 30, 2022. Data based on (National Grid ESO, 2022)	33
Figure 11. Increased inertia. ROCOF and time to UFLS (UK and Australia).....	34
Figure 12. ROCOF estimation using parameters listed in D2.5	34
Figure 13. ROCOF estimation using data about diesel generators in (Sabatini, 2018)	35
Figure 14. Wholesale price profile of Finland for January 2019.....	37
Figure 15. Graphical summary of the decision procedure.	37
Figure 16. State of energy of BESSs (1C) with different power capacities providing virtual inertia as a single service to the power system for 24h [Time index represents time intervals of 0.1 sec].	39
Figure 17. Comparison of energy discharge with the real and constant approximation of the discharge rate.	40
Figure 18. Constant discharge rate as a function of the power capacity of a BESS providing virtual inertia as a single.	40
Figure 19. Optimal power capacity reserved for virtual inertia as a function of the price for virtual inertia based on price.	41
Figure 20. Evolution of the BESS' state of energy over time for January 1, 2019, with a price of virtual inertia of €3/MW/h and €15/MW/h. The third figure shows the evolution of the energy prices.	42
Figure 21. Optimal power capacity reserved for virtual inertia for different months of 2019 as a function of the price for virtual inertia, assuming perfect knowledge of the time-of-use price profile per month [January = month_0] (Results for March and April are not plotted due to missing price data in these months).	42
Figure 22. Maximal percentage deviation of revenues obtained by allocating capacity based on imperfect price estimates (other months in 2019) compared to the optimal revenue in January 2019 as a function of different virtual inertia prices. The optimal revenue in January 2019 has been obtained using the exact price profiles for that month.	43

LIST OF TABLES

Table 1: General product characteristics for participating in flexibility market (frequency control).	17
Table 2: Dynamic enactment of Droop control, VSM and VOC (Vikash Gurugubelli, 2022).	23
Table 3: Summary of inertia technologies and main characteristics.	28
Table 4. Summary of model parameters and data.....	38

LIST OF ACRONYMS

VG	Variable Generation
RES	Renewable Energy Sources
CSP	Concentrated Solar Power
FFR	Frequency Fast Response
ESS	Energy Storage System
ROCOF	Rate Of Change Of Frequency
TSO	Transmission System Operator
FCR	Frequency Containment Reserves
FCP	Frequency Containment Process
FRR	Frequency Restoration Reserve
SOGL	System Operator Guidelines
aFRR	automatic Frequency Restoration Reserve
mFRR	manual Frequency Restoration Reserve
FRCE	Frequency Restoration Control Error
LF	Load Frequency
SCADA	Supervisory Control And Data Acquisition
EMS	Energy Management System
AGC	Automatic Generator Control
PV	Photovoltaic
MV	Medium Voltage
RR	Restoration Reserve
FESS	Flywheel Energy Storage System
MG	Motor Generator
DoD	Depth of Discharge
DC	Direct Current
AC	Alternating Current
VSM	Virtual Synchronous Machine
VOC	Virtual Oscillator Controllers
LCoE	Levelized Cost of Energy
LCoS	Levelized Cost of Storage
PWM	Pulse With Modulation
PLL	Phase Locked Loop
DG	Distributed Generators
BESS	Battery Energy Storage System
CCGT	Combine Cycle

1. INTRODUCTION

For several decades, the world has been changing the way it obtains energy for its development. With large penetration of renewable energy sources, there is now a trend away from conventional power plants based on synchronous machines fed by fossil fuels towards modern power systems based on power electronics.

The continuous increment in energy demand and the high implementation of renewable sources through the grid connection of photovoltaic and wind power plants can affect the stability of the parameters in the electricity grid. These changes are causing a reduction in inertia previously provided by systems based on synchronous machines, which operate at a stable and determined frequency, and provide inertia in the event of a contingency occurring, due to the rotation of the moving parts. This means that in a scenario of high penetration of renewable and variable power sources, it is necessary to apply systems with back-up energy capacity and new contingency control models to ensure the reliability and quality of the power grid.

This document aims to make a study and assessment of the current state of the systems and applications that serve as grid back-up and provide inertia to the electricity system. For this purpose, COBRA and CENTRICA have analysed the current technologies available in the market paying special attention to relevant demonstrator and use cases, bringing the virtual inertia demonstrators to the real power systems. Additionally, EDM has included a basic power grid characterization for justifying the impact and the necessity of developing new alternatives based on virtual inertia, guaranteeing the future higher renewable penetration under stable and secure conditions.

2. INERTIA IN GRID SYSTEMS AND POWER QUALITY

This section aims to analyse the impact of a higher renewable penetration in power systems in terms of power quality and grid stability from a general point of view.

Globally, and according to the *NREL Research Roadmap of Grid-Forming Inverters* (NREL, Research Roadmap on Grid-Forming Inverters, 2020), it is expected that power systems evolution will be oriented to a distributed configuration, maintaining certain parts of conventional synchronous generators, but introducing new renewable sources distributed along the power grid and connected to it through power inverters. This expected evolution will introduce new challenges into the power grid control, due to the progressive substitution of synchronous generators by power inverters which will modify the power system inertia, and consequently new control mechanisms must be introduced in the power grid.

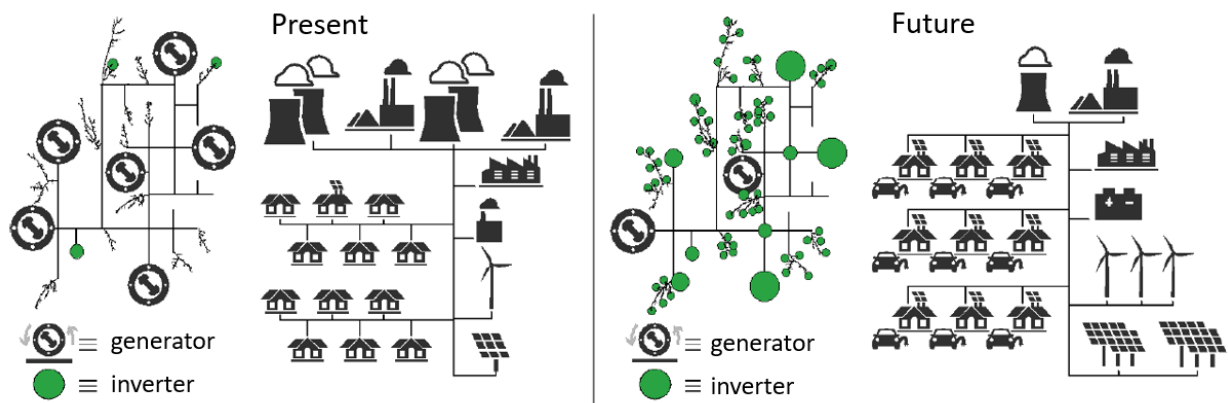


Figure 1. Future direction in the power systems distributions (NREL, Research Roadmap on Grid-Forming Inverters, 2020)

The concept of "inertia" refers to the ability of a system to maintain motion for a period of time until it slows to a complete stop. In the context of a conventional power system, the term inertia literally refers to the rotational inertia in the moving parts of synchronous generators that produce electricity by the electromagnetic effect. The rotational inertia provided by these systems allows stability to be maintained under grid conditions and allows the system to continue to operate for a period of time in the event of contingencies, until the control protocols are triggered. The more inertia a system has, the more stable it can be, the longer the nominal values of the network can be maintained and the slower the rate at which they deviate from their nominal value. The amount of inertia available in a system depends on factors such as the total generation capacity, the technology used for generation, etc.

One of the main benefits of high inertia systems is their ability to withstand changes in frequency, and to dampen their response to power failures. In systems with high-RES penetrations, such as photovoltaic or wind power plants, the conventional inertia available decreases with increasing penetration, as these systems based on variable generation (VG) do not have controllable and stable rotational parts. For this reason, it is necessary to implement alternative systems that complement RES generation, such as power reserves on failure, or virtual inertia systems, which emulate the

behaviour of a synchronous machine in the grid, through the use of grid-forming inverters, and taking advantage of the rapid response of modern batteries.

Some RES power systems that use traditional generators, such as geothermal, hydro, or concentrated solar power (CSP) may add inertia to maintain grid quality, however, variable generation plants such as solar and wind installations do not use traditional generators and therefore do not increase the inertia of the system. The latter can take advantage of the use of grid-forming inverters and batteries to configure Fast Frequency Response (FFR) protocols and thus compensate for the lack of inertia in the system.

Synthetic or virtual inertia refers to the artificial inertia created by the power converter coupled to renewable energy sources. This requires a short-term energy storage system (ESS), a power converter and a real-time control mechanism or algorithm that allows the converter to act like a synchronous generator and provide damping in case of changes in frequency over a short time interval.

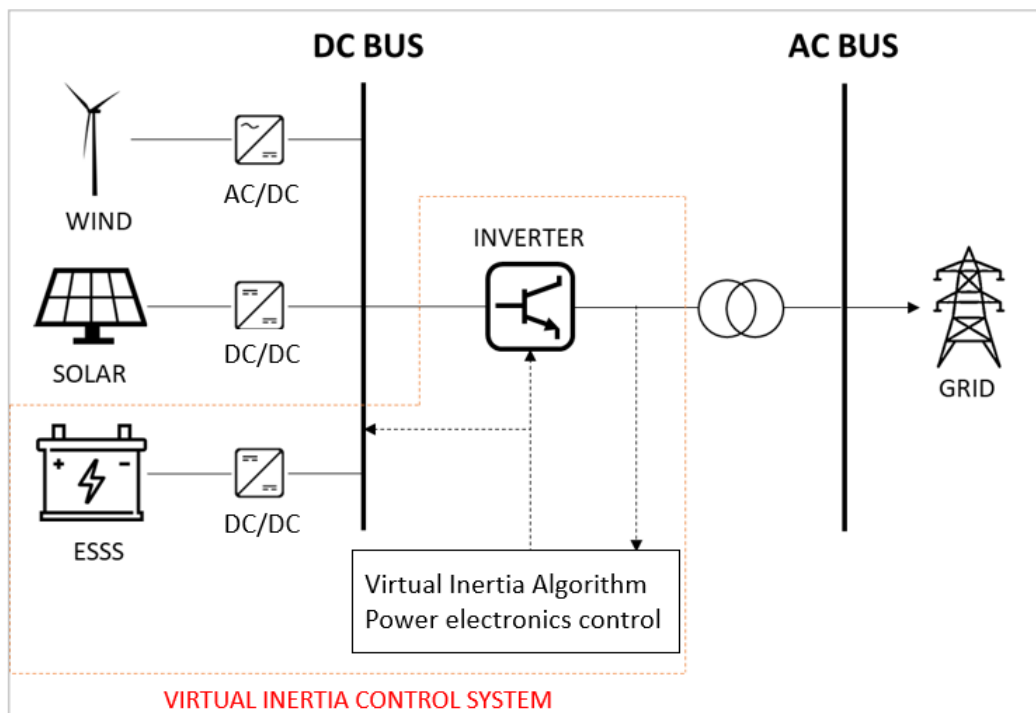


Figure 2. Concept of virtual or synthetic inertia (internal).

Inertia, real or virtual, contributes actively to guarantee the frequency stability and power quality, avoiding high rate of change of frequency (ROCOF) and consequently avoiding damage of equipment (generators, industrial motors, etc.). Issues related to power quality beyond frequency instability are directly related to voltage surges, power outages (even black-out events) and noises.

2.1. REGULATION IN THE EU

To keep the power system frequency within secure limits, Transmission System Operators (TSOs) must maintain the balance between load and generation on a short-term basis according to the instructions published by ENTSOe.

The first step of balancing actions is the application of Frequency Containment Reserves (FCR). These reserves are activated fast (typically within 30s), and they stabilize the power system frequency and make sure that the frequency deviation will not further increase. The Frequency Containment Process (FCP) will stabilize the frequency with an offset from 50 Hz, but it is the change of speed of the rotating masses, inertia, that ensures the frequency change is damped so FCR is able to contain and stabilize the frequency at a value close to 50 Hz.

The second step is assigned to Frequency Restoration Reserves (FRR) which replaces FCR and restores the system to the target frequency. The System Operator Guideline (SOGL) (2017/1485, 2017) – established by Commission Regulation (EU) 2017/1485 of 2 August 2017 – does not demand FRR directly, however, it sets minimum system security, operational planning, and frequency management standards to ensure safety. It also coordinates the system operation across Europe, creating a standardised framework on which regional cooperation, including balancing markets, can be implemented. This SOGL defines two types of FRR: automatic (aFRR) and manual (mFRR). FRR is activated by an automatic control device and/or by manual activation which reduces the Frequency Restoration Control Error (FRCE) to zero value. Usually, the control device for aFRR is called a Load-Frequency Controller (LF-Controller). The LF-Controller is physically a process computer that is implemented in the TSOs' control centre systems (SCADA/EMS/AGC) and collects FRCE measurements every 4-10s as well as providing – in the same time cycle – automated instructions to balancing service providers that are connected by data communication links.

Finally, in the third step, the Frequency Restoration Process (FRP), aFRR and/or mFRR, will restore frequency by replacing the power from the FCR. This principle is applicable for normal imbalances like the switching on of a light bulb, the start of a train or the sudden outage of a large power plant. Market behaviour like the stop and start of production units at hour shifts will also create a power imbalance and result in frequency deviations. All frequency deviations are recorded carefully for further analyses. The SOGL defines processes for the calculation and the evaluation of frequency data and the required parameters for each synchronous area and each LFC block (defined in SOGL in Articles 127 – 131, and in Annex III-V).

The following figure summarizes the different mechanisms for guaranteeing the frequency control in the power system (primary, secondary, and tertiary reserves).

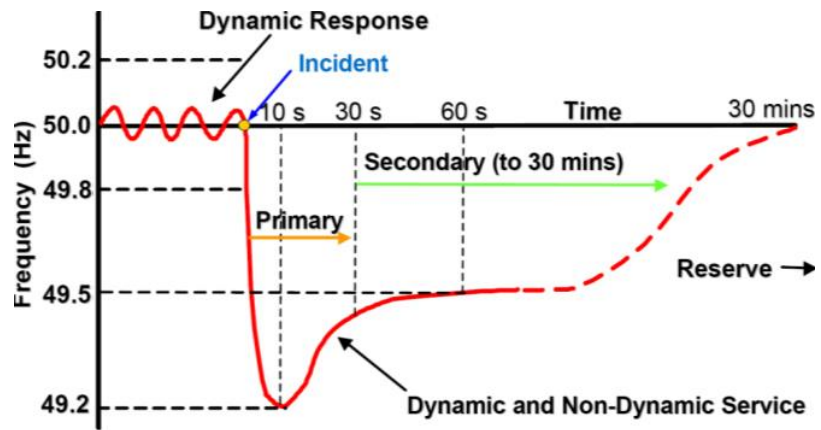


Figure 3. Frequency control mechanisms (Fei Teng, 2016).

3. CASE STUDY – SPECIFIC TO MAYOTTE`S POWER GRID

3.1. CHARACTERISTICS OF MAYOTTE`S POWER GRID

Today the community of Mayotte is involved in an energy transition to decarbonize its electrical generation and its energy sector by the development of renewable sources, specially increasing the installation of solar photovoltaic power plants. Currently, about 95% of the electricity production in Mayotte comes from Diesel generators, and the remaining 5% comes from recently installed RES plants, mainly solar. The current rate of installed PV power plants is 24 MW_p with a 4% annual growing rate.

In April 2017 the latest “Programmation Pluriannuelle de l’Energie” for Mayotte was released; a document setting the objectives, as well as listing the challenges, for the energy policy of the island at different time horizons. To help Mayotte in its energy transition and its decarbonization, the document recommends the following:

- To promote a significant development of RES, especially PV plants, with a multiplication by almost 10 of their shares in the electricity mix. Electricité de Mayotte has received many requests from stakeholders for the connection of new PV plants to the grid, for a total capacity of 43,9 MW_p (8% of which is for a connection to the MV grid).
- To promote the development of thermal renewable energy, which are likely to avoid nearly 20 GWh of electricity consumption annually. The measures include an ambitious development of individual and collective solar water heaters.
- To install storage systems for a total capacity of 29,4 MW by 2023. In this context, two batteries of 7,4 MW and 4 MW for load transfer and frequency control respectively will be installed.
- To develop innovative projects based on renewable energy coupled with storage facilities.
- To secure the electricity supply of the island, by:
 - Keeping a non-intermittent power plant in Petite Terre, as the island hosts critical facilities such as the airport and the hospital
 - Diversifying the generation facilities in Grande Terre and working on the stability of the electricity system. One proposition is to create a 44 MW production facility by 2025. The objective is to cover part of this need with a biomass power plant project (12 MW) and a project combining photovoltaic installations and storage (13 MW), with the remainder covered by a power plant running on light fuel or liquefied petroleum gas.
- To promote clean and sustainable mobility (e-mobility, public transit, maritime transport).

The rising number of PV power plants to be installed and connected to the main grid in Mayotte may increase the difficulty of frequency control. Indeed, PV production is highly dependent on weather conditions that are challenging to forecast (e.g., a passing cloud leads to a decline in PV

production), which may lead to increasing the imbalances between generation and consumption. With an increasing number of PV generation, that will partly replace diesel generators, the ratio of spinning machines in the system will be reduced which also has negative impact on the synchronous inertia of the Mayotte power system. The main balancing service to cope with the frequency deviation currently applied on the island of Mayotte is the “primary reserve” (covering FCR and FRR), which is estimated at 15% of the daily demand and mainly supported by the EDM diesel generation sets of Longoni and Badamiers. For this reason, the generators are limited to operate at 80-85% of their maximal capacity. For the past few years, the primary reserve had not exceeded 8 MW, but this will change soon based on the expected rising demand and increasing RES generation. For those reasons, frequency control has been selected for MAESHA.

Many households in Mayotte have no connection to the main energy grid. Ultimately, the local energy infrastructure suffers from a growing number of illegal connections and energy theft poses major challenges to the local grid operator. These issues can create additional problems to Mayottes main energy grid.

3.2. FINDINGS OF PRECEDING TASKS IN MAESHA

According to D4.1, virtual inertia mechanisms considered in this D5.2 can provide support to the Frequency use case. Furthermore, depending on the energy capacity range of the technologies involved in the virtual inertia mechanisms other use cases, such as Minimization of the peak consumption, can also be affordable.

Load-Frequency control is an ancillary service aiming to retain, recover, and restore the grid frequency to its nominal value following supply-demand imbalances or large contingency event. The types of service can be categorized as the inertia response and a set of primary, secondary, and tertiary response levels of the control chain. The products considered in this deliverable are focused on inertia response, however, due to its flexibility characteristics, configured through the proper combination of storage/RES technologies can provide primary regulation.

Going in detail to the flexibility market design options for geographical islands in D4.1, the products and technologies considered in this document could be considered for participating in the frequency control market through FFR and aFRR. A selection of technical characteristics for participating in this market are considered in the following table (more detailed characteristics can be found directly in D4.1).

Table 1: General product characteristics for participating in flexibility market (frequency control).

Attributes	FFR	aFRR
Product type	Capacity	Capacity and Energy
Non-tripping range (Hz)	46 - 55	46 - 55

State-of-charge management	Post-fault restoration	n/a
Maximum preparation period (s)	n/a	30
Maximum ramping period (MW/s)	n/a	250
Maximum full activation time (s)	<0,4	300
Minimum delivery duration (min)	30	30
Communication activation type	Decentralized	Centralized

D4.1 has identified different potential service providers for solving the lack of inertia issue, highlighting: flywheels energy storage systems, wind power plants, and PV plants and batteries energy storage systems – connected to the grid through the proper power electronic equipment (grid-forming inverters).

4. TECHNOLOGIES AND SOLUTIONS TO INCREASE INERTIA IN GRIDS. MARKET REVIEW.

4.1. TECHNOLOGIES BASED ON ROTATIONAL INERTIA

The purpose of this section is to analyse the current existing alternatives for providing rotational inertia beyond conventional synchronous generators. Flywheels and kinetic inertia from wind turbines solutions are described in the following subsections.

4.1.1. Flywheel energy storage system

A flywheel stores energy using the rotating mass principle. It is a mechanical storage device which emulates the storage of electrical energy by converting it to mechanical energy. The energy in a flywheel is stored in the form of rotational kinetic energy. The input energy to the FESS (fly energy storage system) is usually drawn from an electrical source coming from the grid or any other source of electrical energy. The flywheel speeds up as it stores energy and slows down when it is discharging, to deliver the accumulated energy. The rotating flywheel is driven by an electrical motor-generator (MG) performing the interchange of electrical energy to mechanical energy, and vice versa. The flywheel and MG are coaxially connected, indicating that controlling the MG enables control of the flywheel (A Review of Flywheel Energy Storage System. Technologies and Their Applications. Mustafa E. Amiryar and Keith R. Pullen, 2017).

Despite major developments during their early stages, the utilization of flywheels has not been significant and has declined with the development of the electric grid. However, due to the recent improvements in materials, magnetic bearings, power electronics, and the introduction of high-speed electric machines, FESS have been established as a solid option for energy storage applications.

FESS consist of a spinning rotor, MG, bearings, a power electronics interface, and container or housing. The following Figure 4 shows an example of this technology.

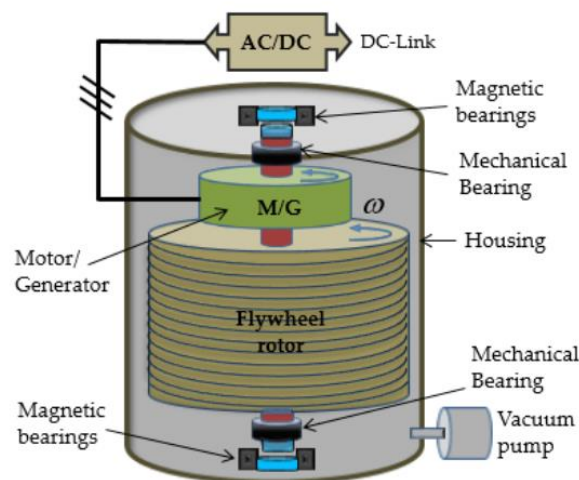


Figure 4. Flywheel scheme (Pullen, 2020).

The specific energy (energy per mass unit) and energy density (energy per volume unit) of a flywheel are dependent on its shape. This shape will determine the flywheel speed limit, and hence, the maximum energy that can be stored. The stored energy basically depends on the spinning speed and the moment of inertia. This allows two types of FESS: low speed (up to 10.000 rpm) and high speed (up to 100.000 rpm). Low speed flywheels are usually made of heavier metallic materials and are supported by either mechanical or magnetic bearings. High speed flywheels generally use lighter but strong composite materials and typically require magnetic bearings. The price of high-speed flywheels can be up to five times higher than the cost of low-speed flywheels.

Regarding the main technical characteristics of FESS the following list summarizes the main aspects:

- High life cycle (hundreds of thousands)
- Long calendar life (more than 20 years)
- Fast response
- High roundtrip efficiency (90-95%)
- High charge and discharge rates
- High power density
- High energy density
- Low environmental impacts

Flywheels have a long lifetime and very low operational and maintenance requirements. The life cycle is also high, compared to many other energy storage systems, as flywheels do not require long charge-discharge cycles. They can be charge and discharge rapidly, based on the application and functionality, and are not affected by the depth of discharge (DoD).

4.1.2. Kinetic inertia from wind turbines

Many modern wind plants can control active power output in response to grid frequency in ways that are important to overall grid performance, but the combined inertia response of a wind power plant will depend on the electrical characteristics of its individual wind turbines. Constant-speed wind turbines have different inertial response in comparison with synchronous generators, however, they do not intrinsically decrease the power system inertia because of their electromechanical characteristics. On the other hand, the rotating mass of variable-speed wind turbines is decoupled from the grid frequency and does not inherently exhibit an inertial response unless controlled for that specific purpose. As a reference, a conventional 1.5 MW variable-speed wind turbine can release up to 200 kW from inertia for 15 seconds when the wind rotors slow down by 5 rpm from the initial speed. With appropriate controls, this turbine inertia can be connected directly to the grid (NREL, Understanding Inertial and frequency response of wind power plants, 2012). This short-term capability of injecting additional power into the grid makes it possible for wind power plants to participate in providing inertial response until the primary frequency control reserve of the power system is activated. Nevertheless, during this period of inertial response, the rotational speed of the wind turbine is decreasing. As a result, the power will drop considerably when the frequency control support is ended. This drop in power will be mostly undesirable, especially when complete wind farms show this behaviour. In larger wind farms, the effect can be mitigated partially by ending the frequency control support of the turbines at different times. Also, a gradual change to normal operation, instead of the abrupt change will improve the global response (IEEE, 2006).

The majority of grid-connected wind turbines in power systems throughout the world are of variable-speed, so enabling controls to provide an emulated inertial response in case of frequency disturbances can become an essential service to the grid, helping to improve minimum frequencies. Such controls are commercially available from some wind turbine manufacturers. Ultimately, grid codes may be modified to include forms of inertial response from wind turbines depending on given utility needs.

4.2. TECHNOLOGIES ANALYSIS BASED ON POWER ELECTRONICS (GRID-FORMING AND GRID-FOLLOWING INVERTERS)

Currently, the majority of existing grid-tied inverters operate as grid-following sources that track the voltage angle of the grid to control their output. Even with inverter fast frequency support, frequency regulation still depends on the remaining synchronous generators. In contrast, grid forming sources actively control their frequency output, enabling them to naturally support the system frequency while sharing a portion of the load change (Pattabiraman, Lassetter, & Jahns, 2018). Considering the approach and applicability of each of these two technologies their differences are analysed in detail below.

A power electronic inverter converts DC power from an energy resource — such as wind, PV, or batteries — to AC power for use in an AC power system. A typical power electronic inverter consists of a DC side, which contains a DC link; a set of switching semiconductor devices; and a grid-side passive filter that prevents switching harmonics from propagating into the grid. The input side of the DC-link interfaces either directly with an energy source or might be connected to additional power electronics-like DC-to-DC converter(s) (NREL, Research Roadmap on Grid-Forming Inverters, 2020).

Because an inverter power stage is built solely with switching devices and passive filters, closed-loop control is required for any kind of meaningful operation. In modern converters, a significant fraction of closed-loop controllers takes the form of a digital controller. Digital controllers are fully programmable, so they exhibit a high degree of algorithmic flexibility and enable the synthesis of new controllers with relative ease.

The first goal of this section is to explore the power system inertia emulation by the energy stored in the grid-following DC-link capacitors connected power converters. Considering that the DC-link capacitors are always necessary in power converters for harmonics filtering and voltage support, the proposed frequency support brings in no extra cost in terms of system hardware, storing the energy in the DC-link capacitors directly. This frequency response through power electronics can be activated in a range from 0,01 s to 0,1s depending on the hardware characteristics, however, this concept of fast frequency response should not be confused with virtual inertia, which is a concept inherent due to the physics of the two interconnected voltage sources, where the impact on frequency regulation is instantaneous.

The second goal is to focus on the frequency control based with power electronics is oriented to grid-forming inverters and their associated controllers. This type of inverter and controllers can regulate instantaneous terminal voltage and can coexist with other grid-following and grid-forming

inverters and synchronous generation on the same system. This contrasts with grid-following units that act as current sources and cannot function without an externally regulated voltage. In principle, grid-forming inverters should allow for the realization of scalable and decentralized AC power systems where system voltages and frequency are regulated by the collective interactions of the grid-forming units themselves. In this sense, the synchronous machine represents the well-understood grid-forming interface (NREL, Research Roadmap on Grid-Forming Inverters, 2020).

This solution allows the connection of renewable sources like photovoltaic technology to the grid providing certain level of grid support, in terms of inertia. In addition, in the case where batteries or supercapacitors are connected to this type of inverter not only does it allow for the immediate support to the grid inertia but also the complete energy dispatchability during a certain period of time depending on the storage technology characteristics and configuration (batteries are limited in power, though present a high storage ratio; on the other hand, supercapacitors have high levels of power with low energy storage ratio).

Grid-forming controllers can be categorized as droop controllers, virtual synchronous machines (often called synchronverters), and/or virtual oscillator controllers (NREL, Research Roadmap on Grid-Forming Inverters, 2020).

- **Droop control:** This constitutes the most common grid-forming method. Its key feature is that it exhibits a linear trade-off between frequency and voltage versus real and reactive power, much like a typical synchronous machine does in steady state.
- **Virtual synchronous machines (VSM):** This approach is based on the emulation of a synchronous machine within the controls of an inverter. Specifically, inverter terminal measurements are fed as inputs into a digital synchronous machine model whose emulated dynamics are mapped to the inverter output in real time. The complexity of the virtual machine can vary greatly, from detailed electromechanical models to simplified swing dynamics.
- **Virtual oscillator controllers (VOC):** In recent years, another inverter control method based on the emulation of nonlinear oscillators has emerged. Much like a virtual synchronous machine, real-time measurements are processed by the digitally implemented model whose output variables modulate the inverter power stage. The key difference is that the model takes the form of an oscillator circuit with a natural frequency that coincides with the nominal AC grid frequency, and its remaining parameters are tuned to adjust the nominal voltage and control the bandwidth.

The main difference between Droop control and VOC methods is related to their dynamic performance. Analytical and experimental results (NREL, Comparison of Virtual Oscillator and Droop Control, 2017) show that the droop control method suffers from inherent limitations in its dynamic performance due to the need of measuring and filtering real and reactive power. In contrast, VOC acts on instantaneous measurements and inherently provides a faster and better damped response. In the same way, VSM imitates the droop characteristics (equivalent to Droop control) and also the swing equation, however, again the feedback signals of voltage and current must be measured to calculate

the averaged real and reactive powers. Consequently, once again the VOC gives a better performance compared to VSM (SYSTEMS, 2021). The following table summarizes the rise and settling times for these three controllers according to the analysis carried out in (Vikash Gurugubelli, 2022).

Table 2: Dynamic enactment of Droop control, VSM and VOC (Vikash Gurugubelli, 2022).

Reference active power	Specifications	Droop	VSM	VOC
+50% Changes	Rise time (ms)	2,51	2,49	0,30
	Settling time (ms)	4,24	4,21	2,41

Despite the differences between droop controllers, virtual synchronous machines, and virtual oscillators, all three methods have similar properties. In particular, the output terminal behaviour of an inverter with any of these grid-forming controllers resembles a voltage source with an amplitude and frequency that varies with reactive power generation and the system load, respectively. This property allows grid-forming inverters to adjust output power nearly instantaneously to balance loads, regulate local voltage, and contribute to frequency control. Although grid-following inverters can be programmed to emulate the aforementioned grid-forming properties, they nonetheless require a well-defined terminal voltage as a reference.

In addition, despite the fact that the converter is the equipment that directly “form” or “follow” the grid, it is usually connected to non-dispatchable renewable sources or batteries. This fact implies important differences. For example, in the case the converter is connected to non-dispatchable renewable sources (basically PV or wind farm technologies), the equipment can only support the grid if the renewable source is available. Additionally, the solar and wind foreseen availability is limited and usually accumulates certain degrees of inaccuracy. However, in the case that the converter is connected to a battery, the energy and power available to the grid has a high certainty and predictability. In contrast, the LCoE (Levelized Cost of Energy) of PV or Wind farm facilities are lower than the LCoS (Levelize Cost of Storage) associated to current batteries.

4.3. VIRTUAL INERTIAL TOPOLOGIES

This section aims to analyse the virtual inertia topology associated to the different grid forming controllers previously mentioned. This analysis considers the way in which constituent parts of the inverter control are interrelated or arranged, showing the schematic control diagrams of each alternative.

Considering the previous categories, the approaches based on droop control try to approximate the behaviour of synchronous generators to improve inertial response of power systems with a high presence of grid-following inverters. The schematic of a frequency-droop controller is shown in the Figure 5, where ω_g is the local grid frequency, P_{in} is the reference set active power, P_{out} is the measured active power output, m_p is the active power droop and ω^* is the reference frequency. This topology assumes that the impedance of the grid is inductive, which constitutes a limitation due to it might not

always be valid. Often a low pass filter with a time constant T_f is used when measuring the output power to filter out high frequency components from the inverter (Ujjwol Tamrakar, 2017).

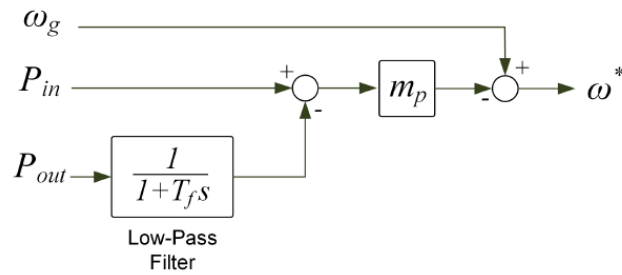


Figure 5. Schematic for frequency droop control (Ujjwol Tamrakar, 2017).

Regarding the synchronverter topology, as mentioned in (Ujjwol Tamrakar, 2017) the Figure 6 shows the basic schematic of the synchronverter topology. According to this scheme the inverter output current i and grid voltage v are the feedback signals used for solving the controller algorithm. On the other hand, moment of inertia, J and damping factor D_p can be fixed as desired, considering their impact on the system stability. The frequency and voltage loops are used to generate the control inputs - the mechanical torque, T_m and $M_f I_f$. In the frequency loop, T_m is generated from the reference active power P^* based on the nominal angular frequency of the grid ω_n . The virtual angular frequency of the synchronverter ω is thus generated by this loop which is integrated to calculate the phase command θ and is used for the pulse width modulation (PWM). Similarly, in the voltage loop, the difference between the reference voltage v^* and the amplitude of the grid voltage v is multiplied by a voltage drooping constant D_q . This is added to the error between the reference reactive power Q^* and the reactive power Q calculated. The resulting signal is then passed through an integrator with gain $1/k_v$ to generate $M_f I_f$. The outputs of the controller are e and θ which are used for PWM generation.

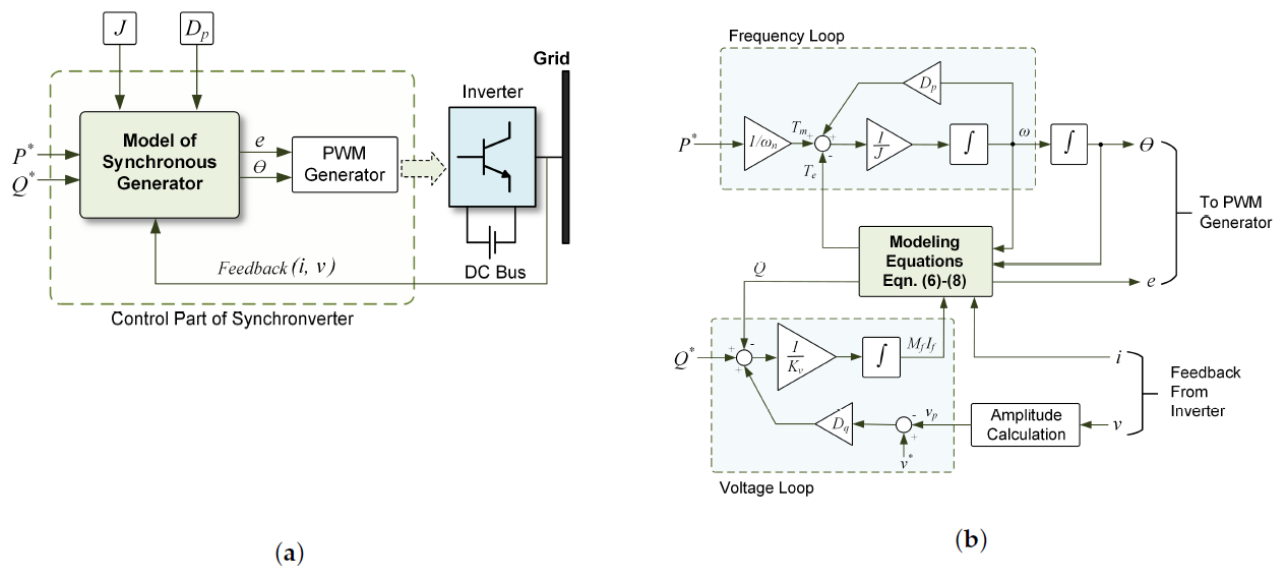


Figure 6. Synchronverter topology: (a) overall schematic showing operating principle; (b) detailed control diagram showing the modelling equations (Ujjwol Tamrakar, 2017).

The basic version of synchronverter requires a PLL (phase locked loop) to initially synchronize with the grid, however the use of PLLs in weak grids is known to be prone to instabilities. To counteract this, self-synchronized have been developed. Moreover, the voltage-source based implementation means that synchronverters can be operated as grid forming units, and ideally suited for inertia emulation from DGs that are not connected with the main grid. The fact that the frequency derivative is not required for the implementation, is a major advantage as derivative terms often induce noise in the system. Although the synchronverter is able to replicate the exact dynamics of a synchronous generator, the complexity of the differential equations used can result in numerical instability. Moreover, a voltage-source based implementation means there is no inherent protection against severe grid transients, which may result in need of external protection systems for safe operation (Ujjwol Tamrakar, 2017).

Finally Virtual oscillator controller (VOC) is another approach where, instead of mimicking synchronous/induction generators, a non-linear oscillator is implemented within the controller to synchronize DG units without any form of communication. This approach is particularly beneficial for a grid largely dominated with DGs, as the controller is intrinsically able to maintain synchronism and share the total system load (Ujjwol Tamrakar, 2017). Figure 7 from (CALIFORNIA, 2018) shows the circuit model of the virtual oscillator and its three parallel components, along with its implementation on a single-phase H-bridge inverter and an LCL filter to reduce high-order harmonics. In this scheme σ represents a negative conductance element; inductance L and capacitance C together yield a resonant frequency of $\omega_{nom} = 1/\sqrt{LC}$; and α governs the magnitude of a cubic voltage-dependent current source. The term v_c denotes the voltage across the virtual capacitor, while i_L refers to the current through the virtual inductor. The term αv_c^3 describes the current consumed by the cubic voltage-dependent current source. To interface with the inverter, k_i scales the current sampled from the inverter's output, and k_v scales the output across the inverter to the nominal voltage magnitude.

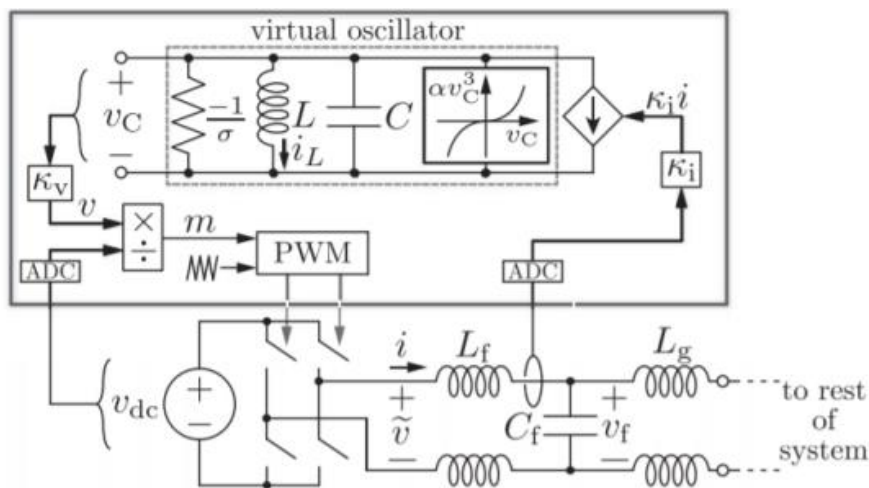


Figure 7. Implementation of VOC on a single-phase H-bridge inverter with an LCL filter (CALIFORNIA, 2018).

Other topologies are available in the literature; however, the basic concept of inertia emulation remains the same in all these techniques.

4.4. DEVELOPED PROJECTS AND EXAMPLES OF APPLICATION

The reduction in inertia is a common problem in islands and geographical islands power systems once renewable technologies like solar or wind farm have an increased presence. Recently, some solutions have been implemented for guaranteeing the required stability of the grid in such scenarios.

M.A.R. project in Canary Islands (Spain) – Flywheel in Tias (Lanzarote Island) (REE, s.f.)

REE launched a system based on flywheel technology that stores energy and acts as a frequency and voltage stabilizer for the Fuerteventura-Lanzarote power system. The installation of this flywheel (with an associated budget of 1.5M€) helps the integration of renewable technologies in the island. This project also pursued the study and analysis of the characteristics of this limited energy storage system through the use of the flywheel, as well as its possible future applications and benefits for both small and larger systems.

The flywheel system which came into operation in August 2014, injects or absorbs energy from the network at a maximum power of 1.65 megawatts (MW) for approximately 12 seconds and provides a total of about 18 MW of electrical power. Likewise, the flywheel system will also allow mitigating the consequences of unexpected changes in the system's frequency within pre-established parameters (50 Hz in Spain), giving its greater stability. In this type of small-sized systems, it is important to maintain frequency and voltage stability, which reduces the response time in the event of power outages.

Dalrymple Battery Energy Storage System (Yorke, Australia) (48, 2020)

The Australian National Electricity Market has experienced a dramatic transformation over the past decade due to the rapid uptake of both small-scale and large-scale renewable energy generation, and the closure of multiple coal power plants. The Australian state of South Australia epitomizes this transformation as the share of renewable energy generation in the state grew from 14% in 2009 to 51% in 2018, dominated by wind power. Combined with limited interstate transmission capacity, the state's power system has experienced instantaneous penetration from wind generation in excess of 140% - the highest for any major power system in the world. This high presence of non-synchronous generation reduces the system strength that has traditionally been provided by synchronous generators.

The Dalrymple Battery Energy Storage System (BESS) (also known as ESCRI-SA) is a 30 MVA / 8 MWh Grid Forming BESS with microgrid automation. It was installed on the lower Yorke Peninsula in 2018, near the end of a long 132 kV single-circuit radial feeder. The Dalrymple BESS is the first (and currently only) large scale, grid forming BESS connected to the NEM (National Electricity Market) and is built on Virtual Synchronous Generator technology. This technology strengthens the grid by replicating the behaviour and performance of a synchronous machine, providing synthetic inertia and high fault current to allow higher levels of renewables to connect and operate [4]. The system also provides reliability and flexibility services such as fast power injection, seamless islanding and black start of the local distribution network. When faults occur on the upstream feeder, the system seamlessly islands in co-ordination with the nearby 91 MW Wattle Point Wind Farm and distributed

solar PV. This allows for continued local islanded power system to operate and ensures continuity of supply to local customers. This makes the Dalrymple BESS more than an energy storage system, but the largest autonomous microgrid in the world.

Virtual Synchronous machine in Dersalloch Wind Park (Scotland)

Following on from smaller-scale investigations of grid-forming converter control applied to wind turbines in 2017-2018, a much larger trial involving an entire wind park, owned and operated by Scottish Power Renewables was produced. The 23-turbine, 69 MW park ran in grid-forming mode for approximately 6 weeks, exploring inertia contributions. A large amount of data was gathered at the turbine and park level, recording responses both to deliberately induced scenarios, and to grid events. Several unscheduled frequency disturbances occurred due to interconnector, CCGT (Combine Cycle Gas Turbine) and other trips, to which un-curtailed turbines were able to actively respond. While a significant amount of incremental improvement (software, hardware, and energy storage) is still required to deal with the most extreme events which could occur, the turbines were able to provide stable and appropriate response at relatively high inertia levels to the frequency events commonly occurring today.

During that time, 6 significant frequency deviation events occurred with ROCOF (Rate Of Change Of Frequency) levels up to ~ 0.1 Hz/s and frequency drops up to ~ 0.5 Hz. The turbines, as a park, were able to respond to all these events, autonomously and immediately, with power responses appropriate to the inertia levels configured. No turbine trips due to issues such as stalling, over-power, or over-current were encountered during the grid events. However, even at the park level, with 23 turbines, natural windspeed fluctuations can cause power output changes of similar magnitudes (and rates of power change) as the typical inertial responses to a 0.1 Hz/s event. The turbines' ability to respond is also extremely small if the turbines are operating at very low powers, or at zero power ("Voltage control mode"). When larger frequency events are considered, for instance 1 Hz/s and 3 Hz drops, the turbines will attempt to respond proportionately, and the windspeed fluctuations will become less significant in comparison. Without additional energy storage, the large events can significantly reduce the rotor speeds and draw the turbines into recovery periods during which their power output is reduced. If not enough wind is available and rotor speeds are initially low, then attempting to provide the full response can slow the rotors below cut-out speed. This reduces power infeed to zero on the turbine(s) affected, which would be the exact opposite of the desired effect. To counter this possibility, one option is to allow the parameterised inertia H to vary in real time, with each turbine offering high H when the wind and rotor speed is appropriate, and a tapered reduction of H when wind and rotor speeds are lower. Although it was not an issue during field testing, a similar tapered reduction of H may be required at high wind/rotor speeds, even though plenty of energy is available. This could be required to avoid the turbine entering an over-power or over-current situation if an additional significant response is required. While dynamic H is a technical option, it presents compliance/market/reward challenges if the provision of inertia directly brings revenue or is required by grid codes. Curtailment and deliberate submaximal power tracking are also options. There are many option permutations for managing all these considerations.

Based on these examples and the references of previous sections the following table summarizes the main characteristics associated to the most relevant solutions for providing virtual inertia.

Table 3: Summary of inertia technologies and main characteristics.

	Maintainability requirements	Performance	Constrains	State of development
Flywheels	Low	90-95%	High power but limited energy	Commercially available
Kinetic inertia from wind turbines	Low	Very high (only mechanical losses)	Provision of inertia implies angular velocity reduction, and output power drop	Test under real environment
Grid forming inverters (connected to RES/Storage)	Low	Very high (~98%)	Limited deployment and untested performance in large power system	Advanced test on microgrids

Considering the previous table, grid-forming inverters, connected to variable renewable sources or storage technologies (batteries), constitutes one of the most promising solutions for guaranteeing the renewable penetration in the power system guaranteeing a stable and secure grid. Its limited cost, high efficiency, low maintenance costs, and promising results position this technology as a very good alternative for complementing the current function of synchronous generators.

4.5. COST COMPETITIVENESS ANALYSIS AND MARKET VALUE OF GRID STABILIZATION

Considering the different alternatives available in the market for contributing to grid-stability through non-inherent inertia systems: flywheels, kinetic inertia from wind turbines, and power electronics supporting RES or storage units; a selection of three realistic configurations (integrating some of these alternatives), based on the analysis carried out in *Power System Inertia: Derivation of Requirements and Comparison of Inertia Emulation Methods for Converter-based Power plants* (Duckwithz, 2019), is detailed below.

This analysis considers three configurations: A) focused on adapting a Wind farm for providing inertia services, B) related to the connection of a battery storage to an existing wind or PV plant, and C) based on a combination of synchronous condenser and a flywheel. As each configuration has different lifetimes due to different equipment and technologies involved, the analysis is based on the annuity method. This method considers investment costs, operation and maintenance costs and loss energy costs along with the useful life of the solution but differentiating them year by year.

In the case of configuration A, focusing on adapting a Wind farm for providing inertia services, the energy storage is directly available from the rotor inertia. In fact, current wind turbines available in the market allow significant over-loading capabilities. However, to determine the exact components that need modifications, adaptations, or substitutions for providing inertia emulation during the wind

farm useful time, requires specific and deeper research at turbine level. For this reason, the referenced analysis considers two scenarios, with a wide range of investment costs and consequently large uncertainty in the final conclusions:

- The optimistic scenario, which considers the reinforcement of the converter and semiconductors subsystems, assumes an initial investment in the new/adapted equipment of 14 €/kW.
- The conservative scenario, where the converter is upgraded and additional reinforcement of the drivetrain is carried out, considers an initial investment of 133 €/kW.

In configuration B, battery storage connected to an existing wind or PV plants, the storage capacities will be directly provided by the battery unit and the converter system upgrade. Again, and due to the variability of battery solutions available on the market and the current cost reduction associated with economies of scale, a range of costs determined by the optimistic and conservative scenario is established.

- The optimistic scenario considers a high-power battery able to provide the required power for 4 minutes, with an associated cost of 8,3 €/kW (based on the assumed cost of 125 €/kWh in energy terms). In this scenario the associated costs for the DC-DC converter are estimated at 18,7 €/kW.
- The conservative scenario considers a high-power battery pack able to provide the required power for 6 minutes, with an associated cost of 27,6 €/kW (based on the assumed cost of 276 €/kWh). In this scenario the associated costs for the converter are estimated in 44,8 €/kW.

Finally, there is configuration C which is based on a combination of synchronous condenser and flywheel. This combination means the synchronous condenser can support reactive power, and the flywheel can contribute to the system inertia, due to the synchronous condensers having a low acceleration time constant (around 2s). Different scenarios have been defined for the flywheel size due to its associated costs and its related energy and power capacities.

- The optimistic scenario considers a synchronous condenser cost of 50 €/kW, while the investment for the flywheel is estimated in 4,5 €/kW in case of higher energy capacity (around 10,7 seconds of rated energy relative to the machine rated power – low robustness) and 1,68 €/kW for lower energy capacity (around 4,0 seconds of rated energy relative to the machine rated power – high robustness).
- The conservative scenario considers a synchronous condenser cost of 100 €/kW, while the investment for the flywheel is estimated at 19,2 €/kW in the case of higher energy capacity and 7,2 €/kW for lower energy capacity.

The following Figure 8 summarizes the specific annual cost for each configuration, considering not only the previously mentioned investment costs, but also, the operation and maintenance costs [17] and costs due to losses in energy [17] along with the useful life of each configuration.

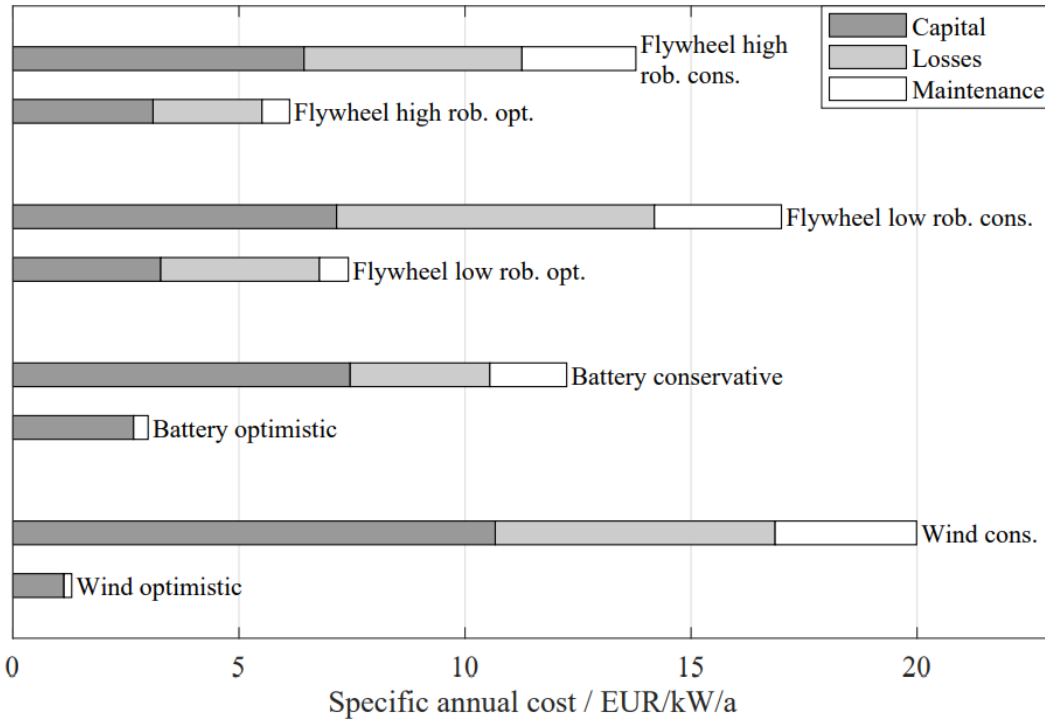


Figure 8. Specific annual cost of inertia for wind, battery, and synchronous flywheel configurations [17].

In general terms, and regarding the previous figure, scenario B has an average lower specific annual cost. However, scenario A offers an interesting alternative with a very high potential for reducing costs, which can be the cheapest if the optimistic scenario is the only one considered. On the other hand, configuration C offers the worst scenario basically due to the relevancy of energy losses, generally associated to the flywheel.

Despite the relevant costs associated with the inertia solutions, it is important to compare them with renewable and conventional energy sources. If the average capital cost of the battery scenario is selected as a reference (5,1 €/kW/a) and a total useful life of the system of 20 years is assumed, the total capital cost for this inertia solution can be considered as around 101 €/kW. This cost represents the 10% (approximately) of the capital cost associated to utility scale PV or Wind farm power plant, based on the references showed in the following figure – extracted from annual LAZARD’s report about Levelized Cost of Energy of renewables sources [17]. Moreover, the summatory of the capital cost of a PV or a Wind farm plant plus this inertia solution is in the range of a gas combined cycle power plant, which is one of the main sources of synchronous generators – and consequently of inertia – in any power system.

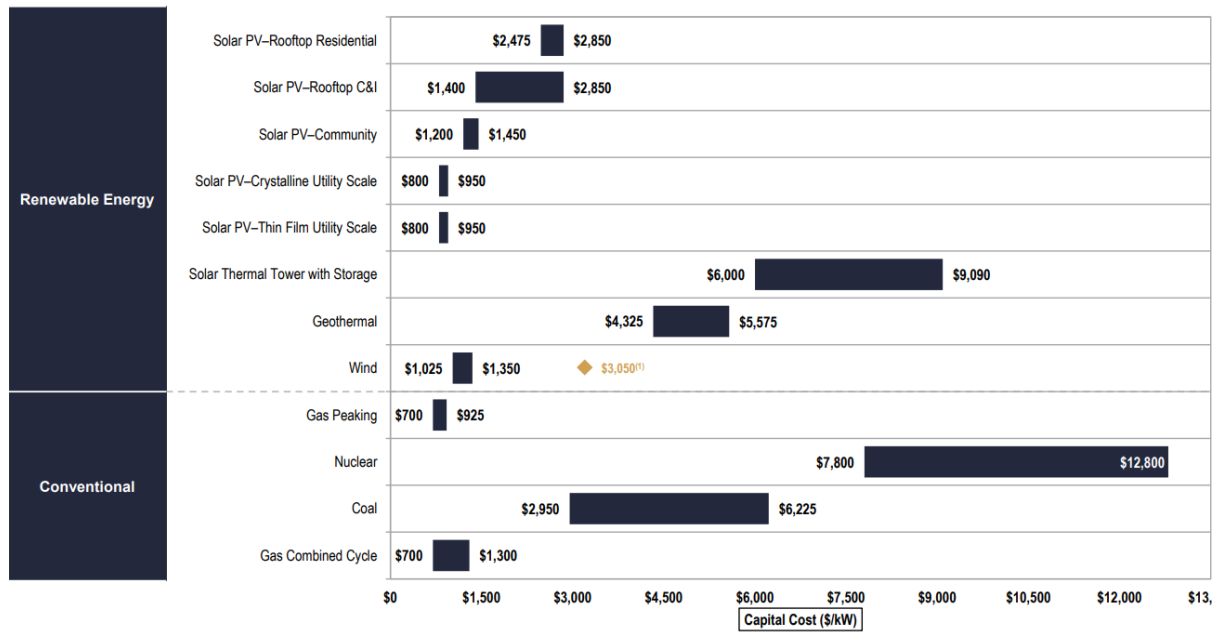


Figure 9. Capital cost comparison for renewable and conventional energy sources [17].

The introduction of inertia solutions will not add new energy capacities to the system, and consequently, the associated Levelized Cost of Energy (LCoE) associated to the renewable power plant incorporating the inertia solutions will increase. However, it will avoid the investment in redundant power plants able to provide real inertia like conventional power plants, contributing to the energy cost reduction. In addition, from the owner assets position, the acquisition of a more stable solution, but also more expensive (renewable power plant + inertia system), will not imply necessarily lower benefits. According to D4.1, services for inertia and fast frequency response can receive a premium payment, as has happen in Ireland, where EirGrid (Irish TSO) procures FFR services that requires response within two seconds and applies a premium payment for response within 0,15 s, which is very close to the inertia concept.

5. THE ROLE OF VIRTUAL INERTIA IN SYSTEM STABILITY

Power system frequency stability is key to prevent blackouts in the system. This concept is linked to the instantaneous balance between demand and supply in the system. If an imbalance exists, the frequency starts to deviate as described by the swing equation, which is well-known in power systems:

$$2. E^I \cdot \frac{d \Delta \bar{f}}{dt} = \Delta P$$

E^I = Inertial response [MVAs]
 ΔP = Power imbalance [MW]
 \bar{f} = Frequency/nominal frequency

In power systems dominated by synchronous generators, the frequency stability is easier to manage as kinetic energy of the rotating mass, i.e., the synchronous inertia, can overcome short periods of imbalance between demand and supply. In power-electronic-converter dominated power systems, this synchronous inertia is much lower and power-electronic interfaced energy resources do not have a natural response to power imbalances. Nevertheless, as discussed in the previous chapters, the power-electronic converters can be controlled in such a way that the inertia of synchronous generators can be mimicked. In this section, we will investigate the importance of virtual inertia to ensure the frequency stability of converter-interfaced power systems.

5.1. MANAGING FREQUENCY STABILITY AROUND THE WORLD

To ensure the stability of their systems, power system operators around the world put constraints on frequency characteristics. The two most popular characteristics to restrict are the rate of change of frequency (ROCOF) and the maximal frequency deviation. In the case the limits of these characteristics are exceeded, the load will be automatically disconnected using protection relays to prevent a full system blackout. To prevent relays tripping, system operators organise their systems by making them resilient against the largest possible loss of generation or load in the system, e.g., the largest generator or the largest interconnector, which may cause the largest ROCOF. The ROCOF in case of an imbalance is also linked to the inertia in the system, i.e., ROCOF = imbalance * nominal frequency / (2 * inertial response). Sufficient inertia should thus be present in the system to prevent ROCOF relays tripping. The frequency nadir is a consequence of the rate of change of frequency and the time before the imbalance is resolved.

While a limit on maximal frequency deviation, or frequency nadir, is applied in most power systems around the world, a limit on rate of change of frequency has mainly been applied in islanded systems on top of the nadir limit. Historically, two main reasons existed to install protection relays with ROCOF limits in the system. First, to avoid pole slipping and catastrophic failure of generating units exposed to ROCOF ranges from 1.5 - 2 Hz/s (over a 500-ms rolling window) (Uijlings, 2013). Second, to prevent embedded generation supplying an electrical island when a loss of mains event has occurred to protect people in the neighbourhood, i.e., anti-islanding protection (Palermo, 2016).

If inertia levels in the system are decreasing, the ROCOF limit has a tremendous impact on the cost-effectiveness of power systems. The system operator needs to take several remedial actions to prevent ROCOF relay tripping by limiting the largest possible loss of generation in the system or by increasing the synchronous inertia connected to the system. To limit the largest possible loss of generation or to increase the inertia in the system, power system operators have to redispatch generation and bring online more expensive generators that were out of the energy market. For the system of Great Britain, the system operator National Grid ESO spent almost 28 million pounds between April 1 and September 30 in 2022 purely for managing the rate of change of frequency within limits. Figure 10 gives the evolution of the costs as a function of time. These numbers are not representative for the system of Mayotte, but give an indication of the cost in a real-life system. To

evaluate the value of virtual inertia for a power system, the net present value of introducing virtual inertia in the system should be evaluated. Assuming that the probability of blackouts with the state-of-the-art approach of redispatch and the alternative approach of virtual inertia remains the same, this entails a calculation of the cost difference between the current approach and the scenario in which virtual inertia is added to the system. For the UK system, this means that using virtual inertia has a positive net present value if its net cost per year is below 28 million pounds. Although this value gives an indication of the costs in a real-life system today, they are not representative for the system of Mayotte. Mayotte is today preventing a significant amount of these issues by putting strict limits on the amount of PV generation that can be integrated in the system. Estimating the true cost of frequency management in the Mayotte system would require relieving the limits on the solar generation.

To reduce this continuous cost of remedial actions, system operators of several islanded energy systems have made successful studies in the last decade to assess the feasibility of relieving the ROCOF limits in their system. Based on these studies, the impact of relieving the ROCOF limit was limited, and they are currently relieving the ROCOF limits in practice, e.g., 0.125Hz/sec to 1Hz/sec in UK and 0.5Hz/sec to 1Hz/sec in Ireland.

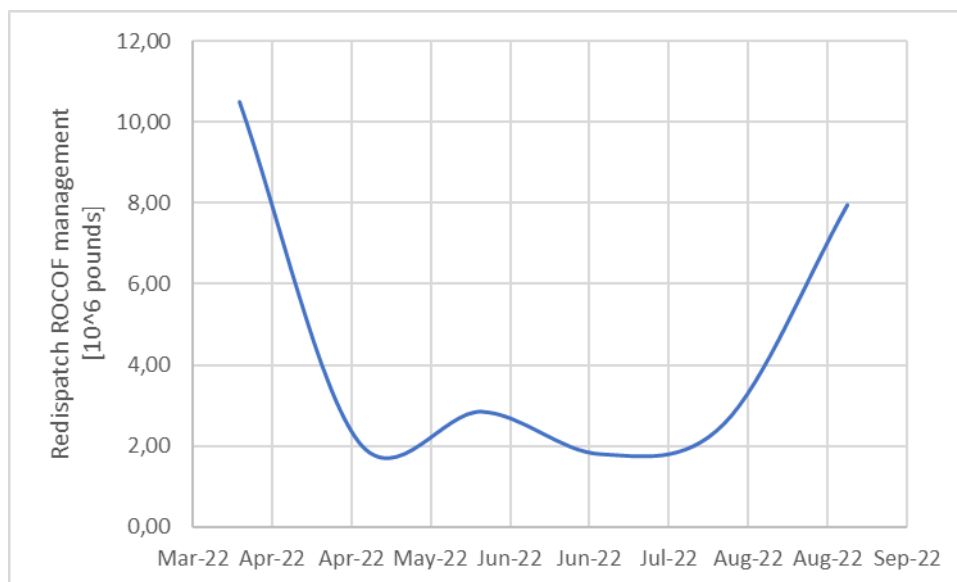


Figure 10. Costs spent on ROCOF management by National Grid between April 1 and September 30, 2022. Data based on (National Grid ESO, 2022)

5.2. ADDED VALUE OF VIRTUAL INERTIA FOR FREQUENCY STABILITY

By relieving or removing the ROCOF limit, higher ROCOFs will occur in the system if the inertia decreases. This results in less time available to prevent underfrequency load shedding. System inertia thus gives the system operator time to react upon a power imbalance. The table below summarizes different ROCOF levels, and thus inertia levels, at the time before underfrequency load shedding takes place according to the UK and Australian nadir limits. The table clearly indicates that very fast response upon a frequency deviation would be needed to prevent underfrequency load shedding.

	ROCOF	Time to UFLS (49.2Hz) UK	Time to UFLS (49Hz) Australia
Increased inertia ↓	4 Hz/sec	0.2 sec	0.25 sec
	2 Hz/sec	0.4 sec	0.5 sec
	1 Hz/sec	0.8 sec	1 sec
	0.5 Hz/sec	1.6 sec	2 sec
	0.125 Hz/sec	6.4 sec	8 sec

Figure 11. Increased inertia. ROCOF and time to UFLS (UK and Australia).

Fast frequency response services are already applied in different countries worldwide, with reaction times up to 0.7 sec in the Nordic countries, for instance. The time to react upon a frequency deviation strongly depends upon the technology used to react upon the imbalance, e.g., start-up times, but also the latency in measurement, detection, processing, filtering and activation. Fast frequency response alone will not be sufficient to keep the power systems of the future stable, however, it can probably reduce the amount of synchronous inertia needed. In the ideal scenario, where virtual inertia can perfectly mimic a synchronous inertial response, the time to respond for fast frequency response can be increased. Unfortunately, some technological challenges are still present from a virtual inertia perspective, as will be discussed in the next subsection.

The figures below show the ROCOF for different power imbalances in a small islanded system with limited synchronous generation. We have used the parameters given in Table 1 of D2.5 for the diesel generators at Mayotte island in Figure 12 and the parameters of the diesel generators listed in (Sabatini, 2018) in Figure 13. In both cases, we assumed that no additional embedded inertial response from other synchronous load or generation is available in the system. Based on this assumption, we see that the loss of the largest 11MW power plant would result in a ROCOF of 6 Hz/sec with the assumptions of D2.5 and in a ROCOF of 2.1 Hz/sec with the parameters of (Sabatini, 2018).

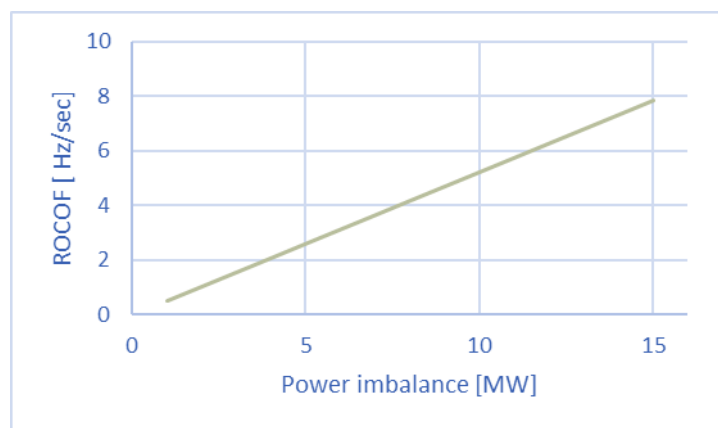


Figure 12. ROCOF estimation using parameters listed in D2.5

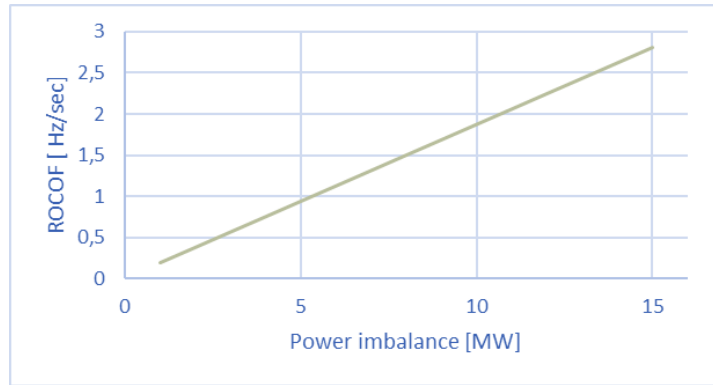


Figure 13. ROCOF estimation using data about diesel generators in (Sabatini, 2018)

Today, the first underfrequency load-shedding limit in Mayotte is 48.5Hz (Sabatini, 2018), which is lower than in the larger systems of the UK (maximal frequency deviation of 49.2Hz) and Australia (maximal frequency deviation of 49Hz). This means that considering the assumptions in D2.5 and a largest loss of 11MW of generation, the underfrequency load-shedding limit is reached within 0,225 seconds. Considering the assumptions in (Sabatini, 2018), this would be in 0,73 sec. The latter time duration lies in the range of current fast frequency response services in other systems. However, reaching this number requires all groups in the Longoni and Badamier power plants to be connected to the system, possibly as a synchronous condenser, or perfect emulation of synchronous inertia with grid-forming control of power-electronics-interfaced assets. The perfect emulation is not yet achievable with these last technologies and the latencies still presented in grid-forming control may cause additional instabilities in the system, which need more study and understanding (National Grid ESO, 2020).

The convenience of deploying new inertia solutions in Mayotte, for increasing its stability and maintain certain grid parameters (like ROCOF) under control, will be even higher once the renewable technologies increase their presence on the island. These two reasons justify the detailed monitoring and characterization of inertia associated to the new solutions and innovative prototypes integrated and validated along the execution of WP8. Special attention should be applied to the battery characteristics, due to this asset (as can be observed in the next section) can be used to delivery virtual inertia as well as the traditional capacities – energy time shifting, peak saving and general frequency control as well as others.

6. ECONOMIC ASSESSMENT OF DELIVERY OF A VIRTUAL INERTIA PRODUCT WITH A BATTERY ENERGY STORAGE SYSTEM

The economic assessment comprises the optimal allocation of the limited power capacity of a battery energy storage system (BESS) to energy arbitrage and to a virtual inertia product. One unit of power capacity can be used either for market arbitrage or for the virtual inertia product. The outcome of the analysis indicates how to optimally use a battery for a dual purpose considering different prices for the virtual inertia product, i.e., (i) reserving capacity to offer virtual inertia at a given price and (ii) using the remaining capacity for energy arbitrage exploiting temporal differences in time-of-use energy prices.

6.1. METHODOLOGY

The objective of the BESS owner is to maximize the revenue. However, the constraints posed by the market characteristics and the battery specifications limit the number of feasible solutions.

6.1.1. Virtual inertia product and market

Virtual inertia will be contracted using bilateral, monthly contracts between the system operator and the BESS owners. The system operator contracts virtual inertia with different BESS owners at a predetermined price for one month. The system operator can choose the price. The BESS owner should guarantee that they can deliver the required power to the system upon request. The requested power changes continuously and is correlated to the rate of change of frequency in the power system. The BESS should react upon the power request in a sub second time scale. The energy provided, i.e., the power provided over a particular time duration, is charged at the imbalance price at the given moment. As the power capacity offered for virtual inertia should be available 100% of the time, the BESS owner should reserve this capacity as a part of the BESS's total power capacity. 100% availability also means that the battery should never run full or empty. A full or empty BESS can be prevented by not bidding 100% of the BESS's power capacity to the virtual inertia product and using the remaining capacity to strategically charge at low time-of-use prices to prevent depletion.

6.1.2. Energy arbitrage with a BESS

Time-of-use energy tariffs provide a price that differs per hour of the day and reflect the variations in energy prices on the wholesale energy market. A monthly price profile is shown for illustrative purposes in Figure 14. In practice, the charge and discharge behaviour of a battery should be scheduled with an hourly resolution if we consider time of use tariffs. If intraday trading is also an option, the resolution would be defined by the clearing interval, e.g. 15 min or 30 min (in France). The battery optimally charges when prices are low and discharges at higher prices. In the charge and discharge process, the power capacity of the BESS is limited, limiting its charging and discharging rate, and the energy capacity is limited, limiting the amount of energy that can be stored.

To determine the optimal charge and discharge schedule, prices are known in advance in the ideal case. However, this is not the case in practice. Nevertheless, in the context of this analysis, i.e., making a monthly decision upon the optimal capacity to reserve for virtual inertia, it is infeasible to accurately forecast the energy prices for the next month with an hourly resolution. For this reason, we consider it a reasonable assumption to use the data of the time-of-use energy prices of the previous month as an estimate.

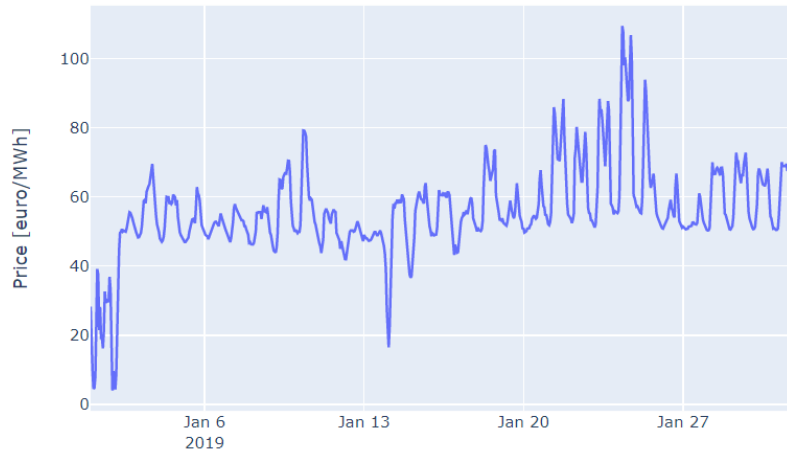


Figure 14. Wholesale price profile of Finland for January 2019.

6.1.3. Optimization model

The optimal capacity allocation is determined using a linear program that considers the market characteristics and battery specifications. One day before the start of each month, the virtual inertia capacity bid needs to be provided. Once the month starts, the power capacity allocated to virtual inertia is reserved to continuously provide virtual inertia to the power system. The real-time power injection or usage is proportional to the real-time rate of change of frequency and is determined based on the real-time frequency signal with sub second resolution. This means that if the frequency is changing with a rate of change of 1 Hz/sec, 100% of the reserved capacity will be activated in real time, while 50% of the reserved capacity is activated with a rate of change of frequency of 0.5 Hz/sec. The remaining power capacity of the battery is used for energy arbitrage to generate revenue and recharge the battery to prevent it running empty. These decisions are taken with an hourly resolution as energy prices change every hour. The decision process is summarized in Figure 15. This procedure is repeated every month.

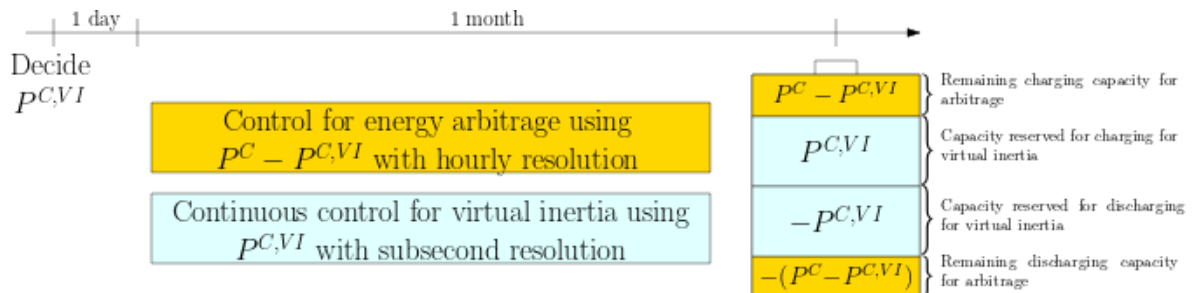


Figure 15. Graphical summary of the decision procedure.

6.1.4. Model parameters and data

Table 4 summarizes the model parameters together with the relevant data source or the value of the parameter used in the analysis. We have used price data of Finland for 2019 given their availability to the company. Originally, these data have been downloaded from nordpool.com. Given the significant changes in energy prices since the beginning of 2021, the results of the analysis will not be generalizable to today. Moreover, in southern power systems such as the one in Mayotte, there is a higher share of PV which leads to lower prices during noon and allows a second charging cycle per day in the arbitrage business. Unfortunately, energy price data for Mayotte were not available for the analysis. Nevertheless, the methodology to get to the conclusions and optimization model used to execute the analysis can be replicated for BESS owners in different contexts.

Table 4. Summary of model parameters and data

Model parameter	Symbol	Unit	Value or source
Charge and discharge efficiency of the battery	η	[/]	0.9
Energy capacity of the battery	E^C	[MWh]	25
Power capacity of the battery	P^C	[MW]	50
Time-of-use energy price in each time interval	π_t^W	[€/MWh]	Data Finland 2019
Imbalance price in each time interval	π_t^R	[€/MWh]	Data Finland 2019
Price of virtual inertia	π^{vi}	[€/MW/h]	Varying between 0 and 60
Number of days in the month	D	[/]	Depending on the month
Number of time intervals in a month	N_t	[/]	$24 \cdot D$
Length of a time interval	Δt	[h]	1
BESS' state of energy at 00:00 each day	S^{init}	[MWh]	12.5

6.1.5. Model variables

The decision variables in this problem statement are:

- The power capacity reserved for virtual inertia: $P^{C,VI}$
- The charging or discharging power for energy arbitrage in a given time interval: $P_t^W \forall t \in [0, N_t]$
- The other variables are:
- The state of energy of the BESS at each time instant throughout the day: $S_t \forall t \in [0, N_t+1]$
- The power capacity reserved for energy arbitrage: $P^{C,W}$
- The charging and discharging energy for virtual inertia in each time interval: $E_t^{VI} \forall t \in [0, N_t]$
- The charging and discharging energy for energy arbitrage in each time interval: $E_t^W \forall t \in [0, N_t]$
- The rate of average energy discharge in the virtual inertia product per 0.1 second time interval as derived based on ex-ante simulations: R based on coefficients a and b

6.1.6. Model formulation

The analysis relies upon a linear program to determine the optimal values of the decision variables:

$$\min -P^{C,VI} \cdot \pi^{vi} \cdot 24 + \sum_{t=0}^{N_t} (E_t^{VI} \cdot \pi_t^R + E_t^W \cdot \pi_t^W) \quad (1)$$

$$\text{subject to } S_0 = S^{init} \quad (2)$$

$$S_k = S^{init} \quad \forall k \in \{24, 48, \dots, 24 \cdot D\} \quad (3)$$

$$S_{t+1} = S_t + E_t^{VI} + E_t^{W,real} \quad \forall t \in [0, N_t] \quad (4)$$

$$0 \leq S_t \leq E^C \quad \forall t \in [0, N_t + 1] \quad (5)$$

$$P^{C,W} = P^C - P^{C,VI} \quad (6)$$

$$0 \leq P^{C,VI} \leq P^C \quad (7)$$

$$-P^{C,W} \leq P_t^W \leq P^{C,W} \quad \forall t \in [0, N_t] \quad (8)$$

$$E_t^W = P_t^W \cdot \Delta t \quad (9)$$

$$E_t^{W,real} = \eta \cdot \max(0, E_t^W) - \frac{1}{\eta} \cdot \max(0, -E_t^W) \quad (10)$$

$$R = a + b \cdot P^{C,VI} \quad (11)$$

$$E_t^{VI} = -R \cdot 60 \cdot \Delta t \cdot 60 \cdot 10 \quad (12)$$

Eq. (1) is the objective function minimizing the cost for the BESS owners. Revenues are considered as negative costs, which explains the minus sign in front of the first term, representing the capacity payment to reserve capacity for the virtual inertia product in the given month. The second term

accounts for the imbalance caused by providing virtual inertia, which is charged at the imbalance cost. The third term represents the costs from energy arbitrage. In general, discharging corresponds with a negative energy and thus a revenue, and charging with a positive energy and thus a cost. Eq. (4) tracks the state of energy throughout the day, considering the charging and discharging to provide virtual inertia or used for energy arbitrage. The stationary losses of the BESS (ca. 1-2% SOC per day) have been ignored in the analysis. Eq. (2) and Eq. (3) ensure that the state of energy of the battery is the same at the start and at the end of the day, which is a common practice in battery energy management. Eq. (5) ensures that the state of energy of the battery is within the energy capacity at each point in time. Eq. (6) defines the capacity assigned to energy arbitrage. Eq. (7) ensures that the capacity assigned to virtual inertia is smaller than the total power capacity of the battery. Eq. (8) ensures that the power used for energy arbitrage is within the power capacity limits assigned for energy arbitrage. Eq. (9) and Eq. (10) calculates the energy charge or discharge due to energy arbitrage in a given time interval. Eq. (11) and Eq. (12) are explained in more detail in the next section, as these require further analysis.

6.1.7. Impact of virtual inertia provision on BESS's state of energy

Eq. (10) and Eq. (11) express the discharge energy to deliver the virtual inertia to the system per time interval Δt . Simulations of batteries with different power capacities delivering virtual inertia considering frequency measurements of the Nordic system, i.e., including Sweden, Norway, Finland and part of Denmark, have shown that a constant discharge rate R is a reasonable assumption, i.e., that the evolution of state of energy of a BESS providing virtual inertia follows a linear function of time. Figure 16 shows the evolution of the state of energy of batteries with different power capacities over time, which indicates this linear trend. Figure 17 indicates the accuracy of assuming a constant discharge rate, by comparing the true discharge with a linear approximation. Expressing the slope coefficient of this linear trend, which represents the constant discharge rate, as a function of the power capacity used for virtual inertia also indicates a linear relation, as shown in Figure 18. This relation corresponds with the linear model: $R = a + b \cdot P^{C,VI}$, as used in Eq. (10). The simulations executed to derive these relationships have a resolution of 0.1 second, due to the high resolution of the frequency data. To obtain the energy discharge for virtual inertia per time interval in the optimization model, energy discharge per 0.1 second interval is multiplied by the number of 0.1 second intervals in the time period Δt of 1 hour in Eq. (11).

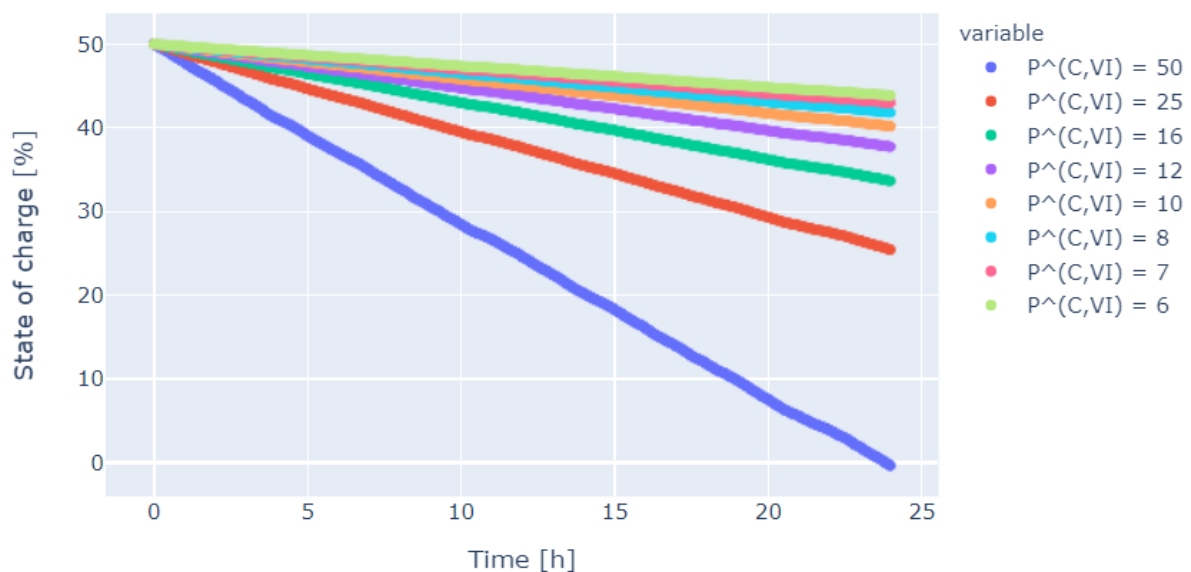


Figure 16. State of energy of BESSs (1C) with different power capacities providing virtual inertia as a single service to the power system for 24h [Time index represents time intervals of 0.1 sec].

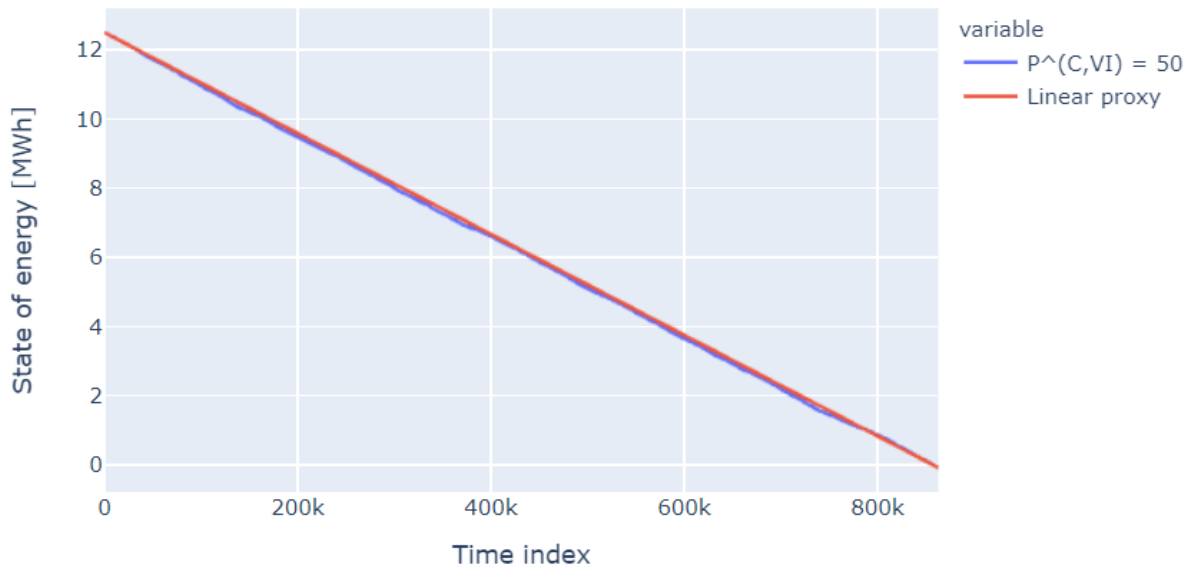


Figure 17. Comparison of energy discharge with the real and constant approximation of the discharge rate.

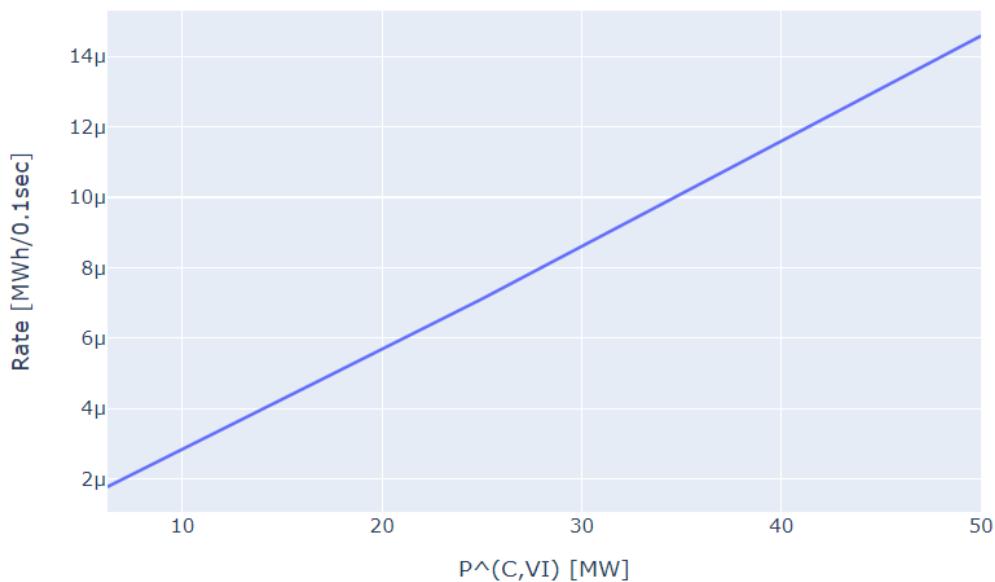


Figure 18. Constant discharge rate as a function of the power capacity of a BESS providing virtual inertia as a single.

6.2. RESULTS

The optimization model gives, for a given price of virtual inertia and a given market price profile, the part of the BESS' total power capacity to assign to the virtual inertia product to maximize the total revenue, if the remaining part is used for energy arbitrage.¹ As the virtual inertia product has not been launched yet, the price of virtual inertia is not exactly known. For this reason, we repeated the

¹ As we do not have price data available for Mayotte island, we restricted ourselves to illustrating the methodology for interpreting the results using a simulation model with limited computational burden. The computational burden has been limited by assuming a 100% efficiency for energy arbitrage which prevents binary variables in the optimization formulation. This assumption results in a worst-case outcome of the business case for virtual inertia, as in practice losses in energy arbitrage will be larger than considered in the analysis.

optimization for different prices of the virtual inertia product to assess how the power capacity assigned to the virtual inertia product varies with the price of virtual inertia.

Assuming perfect information about the market price profiles, the optimal power capacity to allocate to the virtual inertia product at a given price can be obtained. This result is summarized in Figure 19, showing the power capacity to reserve for the virtual inertia product, considering time of use and imbalance price of January 2019. If the price of virtual inertia equals 10 €/MW/h, 98.6 % of the total capacity should be reserved for the virtual inertia. This rises to maximally 98.83 % beyond a price of 13€/ /MW/h. 1.17 % of the power capacity should always be reserved for recharging purposes, to prevent the battery running empty. Even at a virtual inertia price of zero, reserving capacity for virtual inertia is beneficial, i.e., the y-axis does not start from zero. This is caused by excessively high imbalance prices up to €3000/MW/h at certain points in time. At these moments, BESS owners are highly paid to provide only a small amount of virtual inertia to the system, which they eagerly do even if they are not paid to reserve their capacity. Obviously, the imbalance prices have a major impact on the model but are difficult to forecast. This outcome stresses the importance of carefully following up trends in the energy markets and executing the analysis with up-to-date price data in a practical context.

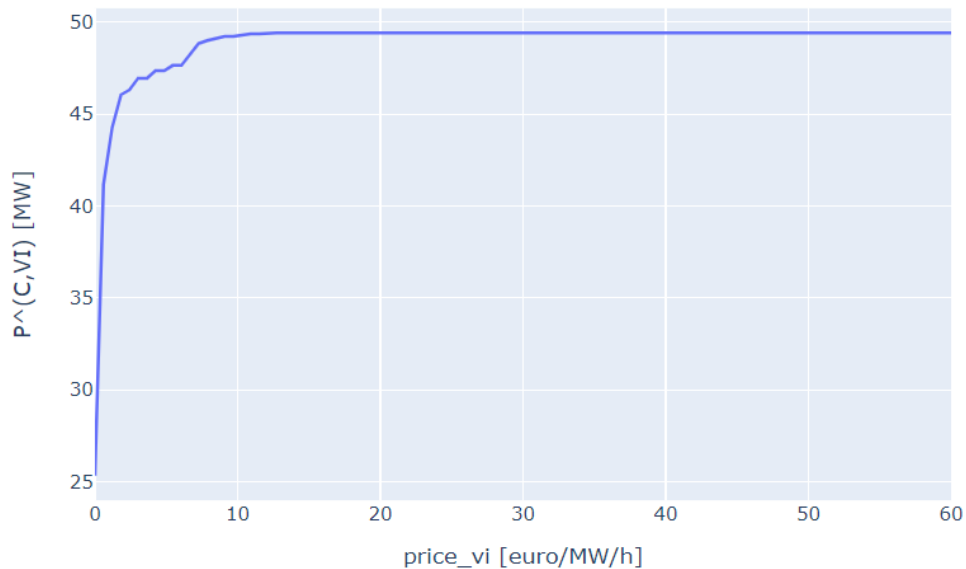


Figure 19. Optimal power capacity reserved for virtual inertia as a function of the price for virtual inertia based on price.

To verify the outcomes of the charging and discharging behaviour of the battery, Figure 20 illustrates the state-of-energy profile of the BESS and the time-of-use prices for a single day, if the virtual inertia price is low (€3/MW/h) and high (€15 /MW/h). The state of energy of the BESS at the start and end of the day equals 12.5 MWh, satisfying the equality constraints in Eq. (2) and (3). Depending on the power capacity allocated to energy arbitrage, the state of energy will vary more (low virtual inertia price, €3/MW/h) or less (high virtual inertia price, €15/MW/h). However, in both cases, the state of energy rises if energy prices are in a valley (charging) and it decreases if energy prices are at a top (discharging), confirming the correct behaviour of the optimization model.

To assess the variability on the results for different time periods, the analysis has been repeated for multiple months. The results show that beyond a virtual inertia price of €20/MW/h, the differences in allocated capacity are small. Below this price, differences in allocated capacity can be observed. The differences are caused by variations in volatility of the time of use prices between the different months. As more volatile prices create a more interesting opportunity for energy arbitrage, the

optimal capacity allocated to virtual inertia at a given price will be slightly lower in months with more volatile time-of-use prices.

To verify the robustness of the solutions with respect to variations in price profiles, the sensitivity of the results to variations in price profiles is assessed. This is done by first solving Eq. (1)-(11) while using the price profiles for every month except January, and then using the resulting allocated power capacity to simulate the revenues for the price profile of the month of January. The result of this simulation is compared against the optimal solution for January with perfect knowledge of the price profiles. The maximum of all deviations is plotted as a function of the virtual inertia price in Figure 22. As can be seen, the maximum of all deviations between the optimal and sub-optimal solutions is approximately 1 %. Based on this result, we can conclude that the sensitivity of the outcomes to the applied price profiles is low. Therefore, we conclude that, for any month, allocating a power capacity within the range of solutions shown for all months in Figure 21 will result in a near-optimal solution.

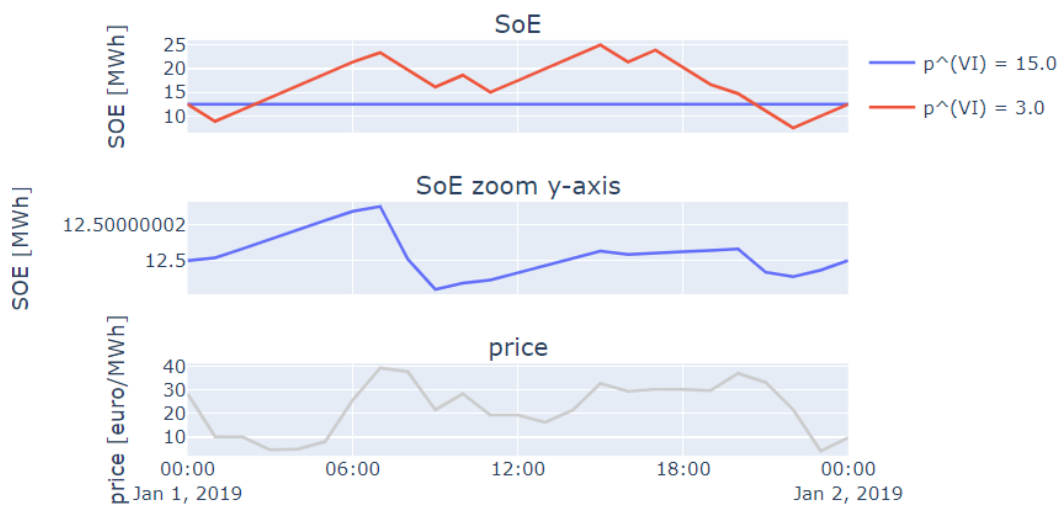


Figure 20. Evolution of the BESS' state of energy over time for January 1, 2019, with a price of virtual inertia of €3/MW/h and €15/MW/h. The third figure shows the evolution of the energy prices.

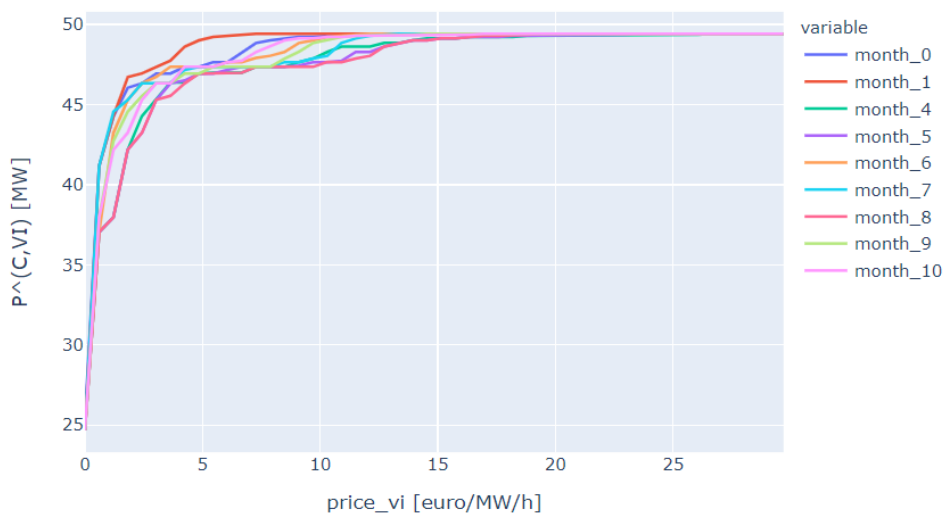


Figure 21. Optimal power capacity reserved for virtual inertia for different months of 2019 as a function of the price for virtual inertia, assuming perfect knowledge of the time-of-use price

profile per month [January = month_0] (Results for March and April are not plotted due to missing price data in these months).

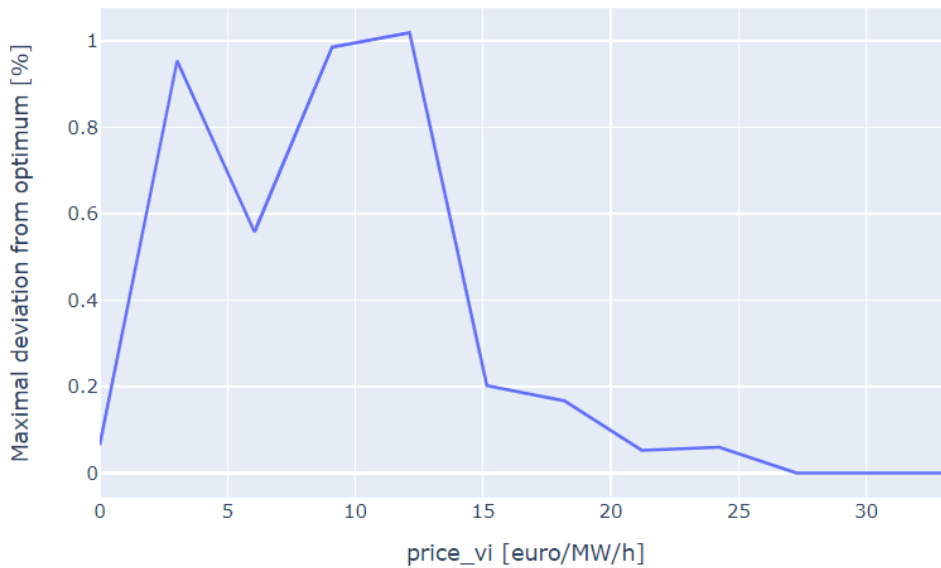


Figure 22. Maximal percentage deviation of revenues obtained by allocating capacity based on imperfect price estimates (other months in 2019) compared to the optimal revenue in January 2019 as a function of different virtual inertia prices. The optimal revenue in January 2019 has been obtained using the exact price profiles for that month.

As a summary, the decision process to allocate the limited power capacity of a BESS to a virtual inertia product and to energy arbitrage while maximizing the total revenue, can be formulated as a linear program in a simplified version to perform an economic assessment. The presented methodology allows BESS owners to determine an appropriate power capacity allocation at different price levels of virtual inertia, as the price of virtual inertia is not yet known. The methodology is applied to price profiles of Finland for 2019. The optimal power allocation is not achievable in practice, as this requires perfect knowledge of the imbalance and time-of-use price profiles, which are not known at the moment of decision making. Nevertheless, a sensitivity analysis using price profiles of different months to determine the allocation in a given month has confirmed the robustness of the methodology, showing a maximal deviation of 1% compared to the optimal solution for different virtual inertia prices. The results show that in January 2019, the power capacity allocated to virtual inertia can vary within a specified range if the virtual inertia price is below €15/MW/h. If the virtual inertia price rises beyond €15/MW/h, the BESS owner should reserve 98.83% of the total BESS power capacity for virtual inertia. This is the maximum power that can be reserved for virtual inertia to keep sufficient power capacity to recharge the BESS, ensuring compliance to a 100% availability of power capacity for the virtual inertia product.

7. CONCLUSIONS

As mentioned in several sections of this document, a high renewable power penetration (PV and Wind Park technologies) in power systems increments the grid instability, and consequently reduces the power system security. In isolated or poorly interconnected power systems, like islands or geographical islands, this issue is critical due to the lower inertia capacities and deserves special attention.

Besides conventional synchronous generators for grid stabilization new solutions are being currently explored on the market. Some of these solutions are based on rotating masses and others on virtual inertia generators. Considering this last concept, it is relevant to differentiate between technologies based on fast frequency response and thoughts for virtual inertia. This is due to the fact that some technologies based on power electronics can provide a fast response for supporting frequency control, however, its response is not instantaneous, and therefore there is a delay that differentiates its response and its capacities for grid frequency support from the inherent inertia response of specific equipment.

Virtual inertia systems and extracting kinetic energy from wind parks seems to provide very promising solutions to the increase in RES penetration and provide flexibility in the grid, but today the technology is still in its early stage of maturity and there are not so many solutions in the market. On the other hand, flywheel technology can provide real inertia and its usefulness has been demonstrated in the demo cases deployed around the world; however, its conventional use requires more research and innovation efforts for reducing its costs.

Furthermore, one of the most promising technologies for virtual inertia support are grid-forming inverters. They have demonstrated their capabilities for contributing to the grid stabilization in an equivalent way to synchronous generators in several demonstration projects. Currently, inverter controls are predominantly grid-following, however, future power systems will involve a combination of both technologies, grid-following, and grid-forming controllers. This ratio between both controllers will depend on how well grid-forming inverters perform and what advantages they will bring to the power grid. Additionally, other important aspects like grid-forming inverter costs (higher than grid-following) and potential statements from grid operators for the mandatory use of these inverters could potentiate their penetration in the power grid.

Different inertia solutions studied from a cost competitive point of view have an associated specific annual cost in the range of 1,3 to 20,0 €/kW/a. In detail, one of the most promising solutions, battery storage system, has an average cost of 5,1 €/kW/a for a total useful life of 20 years, with a CAPEX of 101 €/kW. This cost represents around the 10% of the CAPEX associated to a new PW or Wind farm power plant, in terms of €/kW installed. Despite the inertia solutions not adding high energy capacities to the power system, they avoid the investment needed in redundant power plants able to provide real inertia like conventional power plants and therefore contribute to the energy cost reduction of the power system.

Considering the added value of virtual inertia for frequency stability in Mayotte island, it is important to remark that the loss of the largest 11MW power plant would result in a ROCOF of 6

Hz/sec based on the assumptions of D5.2 and 2.1 Hz/sec if parameters of (Sabatini,2018) are considered. It implies that the underfrequency load-shedding limit would be reached in a range of 0,255 s to 0,72 s, which reinforces the evidence for deploying new inertia solutions in the island, not only for supporting its current operation, but also for guaranteeing the stable operation while the renewable penetration is increasing in the power system.

Finally, regarding the hypothetical use of a BESS for simultaneous services of energy arbitrage and virtual inertia, it can be concluded that if the virtual inertia price rises beyond €15/MW/h, the BESS owner should reserve at least 98% of the total BESS power capacity for virtual inertia. This is the maximum power that can be reserved for virtual inertia to keep sufficient power capacity to recharge the BESS, ensuring compliance to a 100% availability of power capacity for the virtual inertia product. These results are conditioned by the dependency of the results on market price profiles and the high impact of the imbalance price, which are not known beforehand, however, it provides a general view of the importance of selecting the better uses of the battery for maximizing the economic benefits associated to its operation.

8. REFERENCES

- [1] NREL, Research Roadmap on Grid-Forming Inverters, 2020.
- [2] C. R. (. 2017/1485, «Guideline on electricity transmission system operation,» 2017.
- [3] Y. M. Fei Teng, «Challenges of Primary Frequency Control and Benefits of Primary Frequency Response Support from Electric Vehicles,» 2016.
- [4] A Review of Flywheel Energy Storage System. Technologies and Their Applications. Mustafa E. Amiryar and Keith R. Pullen, 2017.
- [5] M. E. A. a. K. R. Pullen, «Analysis of Standby Losses and Charging Cycles in Flywheel Energy Storage Systems,» 2020.
- [6] NREL, Understanding Inertial and frequency response of wind power plants, 2012.
- [7] IEEE, Wind turbines emulating inertia and supporting primary frequency control., 2006.
- [8] D. Pattabiraman, R. H. Lasseter y T. M. Jahns, «Comparison of Grid Following and Grid Forming Control for a High Inverter Penetration Power System,» 2018.
- [9] NREL, «Comparison of Virtual Oscillator and Droop Control,» 2017.
- [10] E. E. SYSTEMS, «Implementation and comparison of droop control, virtual synchronous machine, and virtual oscillator control for parallel inverters in standalone microgrid,» 2021.
- [11] A. G. a. A. K. P. Vikash Gurugubelli, «Parallel inverter control using different conventional control methods and an improved virtual oscillator control method in a standalone microgrid,» 2022.
- [12] D. S. M. M. B. P. B. T. M. H. a. R. T. Ujjwol Tamrakar, Virtual Inertia: Current Trends and Future Directions, 2017.
- [13] U. O. CALIFORNIA, Virtual Oscillator Controlled Inverters in a Microgrid Setting, 2018.
- [14] REE, «<https://www.ree.es/es/sala-de-prensa/notas-de-prensa/2014/10/red-electrica-pone-en-servicio-en-lanzarote-un-volante-de-inercia>,» [En línea].
- [15] C. S. 48, «Grid Forming Energy Storage System addresses challenges of grids with high,» 2020. [En línea].
- [16] D. Duckwithz, «Power Ssystem Inertia. Derivation of requirements and comparison of inertia emualtion methods for converter-based power plants,» 2019.
- [17] LAZARD, «Lazard's levelized cost of energy analysis - version 15.0,» 2021.
- [18] S. G. I. S. Power, «Practical Experience of Operating a Grid Forming Wind Park and its Response to System Events».